(2)

AD-A250 852

WL-TR-91-3076

WRIGHT LABORATORY

INVESTIGATION OF A RELATIONSHIP BETWEEN UNIAXIAL AND BIAXIAL CHEMICAL STRESS CRAZING OF CAST ACRYLIC

Daniel R. Bowman

University of Dayton
Research Institute
Dayton, Ohio 45469-0110

January 1992

Interim report for period January 1990 - December 1990

Approved for public release; distribution is unlimited.

FLIGHT DYNAMICS DIRECTORATE
WRIGHT LABORATORY
AIR FORCE SYSTEMS COMMAND
WRIGHT-PATTERSON AIR FORCE BASE, OHIO 45433-6553

NOTICE

This technical report has been reviewed and is approved for publication.

Tong C. Choe

TONG C. CHOE, 1Lt, USAF
Project Engineer
Windshield System Program Office

Ralph J. Speelman

RALPH J. SPEELMAN
Chief, Aircrew Protection Branch
Vehicle Subsystems Division

FOR THE COMMANDER

Richard E. Colclough, Jr.

RICHARD E. COLCLOUGH, JR.
Chief
Vehicle Subsystems Division

UNCLASSIFIED
SECURITY CLASSIFICATION OF THIS PAGE

REPORT DOCUMENTATION PAGE

Form Approved
OMB No. 0704-0188

1a. REPORT SECURITY CLASSIFICATION UNCLASSIFIED	1b. RESTRICTIVE MARKINGS
2a. SECURITY CLASSIFICATION AUTHORITY	3. DISTRIBUTION / AVAILABILITY OF REPORT Approved for public release; distribution is unlimited.
2b. DECLASSIFICATION / DOWNGRADING SCHEDULE	
4. PERFORMING ORGANIZATION REPORT NUMBER(S) UDR-TR-90-127	5. MONITORING ORGANIZATION REPORT NUMBER(S) WL-TR-91-3076
6a. NAME OF PERFORMING ORGANIZATION University of Dayton Research Institute 6b. OFFICE SYMBOL (If applicable)	7a. NAME OF MONITORING ORGANIZATION Flight Dynamics Directorate (WL/FIVR) Wright Laboratory Air Force Systems Command
6c. ADDRESS (City, State, and ZIP Code) 300 College Park Avenue Dayton, Ohio 45469-0110	7b. ADDRESS (City, State, and ZIP Code) Wright-Patterson AFB, OH 45433-6553
8a. NAME OF FUNDING/SPONSORING ORGANIZATION 8b. OFFICE SYMBOL (If applicable)	9. PROCUREMENT INSTRUMENT IDENTIFICATION NUMBER F33615-84-C-3404
8c. ADDRESS (City, State, and ZIP Code)	10. SOURCE OF FUNDING NUMBERS

PROGRAM ELEMENT NO.	PROJECT NO.	TASK NO	WORK UNIT ACCESSION NO.
64212F	1926	01	12

11. TITLE (Include Security Classification)
Investigation of a Relationship Between Uniaxial and Biaxial Chemical Stress Crazing of Cast Acrylic

12. PERSONAL AUTHOR(S)
Bowman, Daniel R.

13a. TYPE OF REPORT	13b. TIME COVERED	14. DATE OF REPORT (Year, Month, Day)	15. PAGE COUNT
	FROM 90JAN TO 90DEC	January 1992	50

16. SUPPLEMENTARY NOTATION

17. COSATI CODES

FIELD	GROUP	SUB-GROUP

18. SUBJECT TERMS (Continue on reverse if necessary and identify by block number)
Craze Initiation; Uniaxial Stress; Biaxial Stress; Chemical Craze Testing; Cast Acrylic; Isopropyl Alcohol

19. ABSTRACT (Continue on reverse if necessary and identify by block number)
Chemical crazing is directly responsible for many aircraft transparency removals. Laboratory chemical stress craze testing can be used to evaluate the effects of different chemicals on aircraft transparencies. Most craze testing to date has been uniaxial, while the stress state in an installed aircraft transparency is biaxial. The uniaxial craze test is easier to conduct and requires less and more simple fixturing than the biaxial craze test. It is desirable to be able to use uniaxial data to predict the effects of a biaxial stress field on crazing. An experimental program was conducted to develop a relationship between uniaxial and biaxial chemical stress crazing of aircraft grade cast acrylic with isopropyl alcohol. ASTM Standard Test Methods F484 and F1164 were used as guidelines for the uniaxial craze testing and biaxial craze testing, respectively. Time to craze as a function of stress level was determined and used to develop relationships between uniaxial and biaxial crazing in the form of craze initiation criterion, utilizing theoretical and empirical equations.

20. DISTRIBUTION / AVAILABILITY OF ABSTRACT ☒ UNCLASSIFIED/UNLIMITED ☐ SAME AS RPT. ☐ DTIC USERS	21. ABSTRACT SECURITY CLASSIFICATION
22a. NAME OF RESPONSIBLE INDIVIDUAL Mr. Russell E. Urzi	22b. TELEPHONE (Include Area Code) (513) 255-6524 — 22c. OFFICE SYMBOL WL/FIVR

DD Form 1473, JUN 86 — Previous editions are obsolete. — SECURITY CLASSIFICATION OF THIS PAGE

PREFACE

The efforts reported herein were performed by the Aerospace Mechanics Division of the University of Dayton Research Institute (UDRI), Dayton, Ohio, under Air Force Contract F33615-84-C-3404, modification P00011. The program was sponsored by the Wright Laboratory, Flight Dynamics Directorate, Wright-Patterson Air Force Base, Ohio. Air Force administrative direction and technical support were provided by Capt. Paul Kolodziejski and Mr. Russell E. Urzi, WL/FIVR.

The work described herein was conducted during the period January 1990 to December 1990. University of Dayton project supervision was provided by Mr. Dale H. Whitford, Supervisor, Aerospace Mechanics Division, and Mr. Blaine S. West, Head, Structures Group. Mr. D. R. Bowman was the Principal Investigator.

CONTENTS

FIGURES

FIGURES (Continued)

TABLES

SECTION 1

INTRODUCTION

1.1 BACKGROUND

The US Air Force has been and continues to be concerned with aircraft transparency life-cycle costs and overall durability. As part of this concern, the Air Force has funded programs to study transparency materials, evaluate transparency durability, and develop durability test methods. Acrylic plastics are frequently used for aircraft transparencies. Acrylic is subject to a phenomenon known as crazing. Crazes appear to be small cracks in the surface of the material, although they are not. Crazing is a form of yielding in polymers characterized by a spongy void filled fibrillar structure. The density of the material in the craze changes, causing a change in the index of refraction, which causes light to be reflected off of the crazes. Crazing occurs when tensile stresses are present, and is accelerated under the presence of certain chemicals and when temperature is increased. Crazing generally occurs perpendicular to the direction of the largest principle tensile stress.[1] The significance of crazing of acrylic is that it degrades transparency optics and often is the cause for transparency removal and replacement.

The current method of evaluating transparency durability, specifically concerned with chemical craze resistance, is the uniaxial cantilever beam craze test (reference ASTM F 484). This test method has been used almost exclusively in the transparency industry. The advantages of the cantilever beam craze test are that it is simple, it requires minimal equipment, and it is relatively inexpensive. The disadvantage of the cantilever beam craze test is that it does not simulate real world stress conditions. Aircraft transparencies are typically under a biaxial state of stress. A chemical craze test has been developed to evaluate the effect of biaxial stresses on crazing, using a circular plate with clamped edges and a uniform pressure load. While this biaxial craze specimen is more simple to fabricate, test, and analyze than those used by other researchers to study biaxial crazing, the test is more complicated and more time consuming than the uniaxial craze test and requires special fixturing.

1.2 OBJECTIVE

The objective of this test program is to investigate the relationship between uniaxial and biaxial chemical stress crazing of cast acrylic, and to develop a better understanding of the crazing phenomenon. The development of a relationship between uniaxial and biaxial crazing would validate the use of the inexpensive uniaxial chemical craze testing to evaluate the effects of various chemicals on aircraft transparencies.

SECTION 2

TECHNICAL APPROACH

2.1 SCOPE

This program consisted of craze initiation theory development and craze testing. A series of uniaxial and biaxial craze tests was conducted at various stress levels in conjunction with isopropyl alcohol. Isopropyl alcohol was the chosen chemical craze agent because it is a representative chemical which is often used for cleaning of aircraft transparencies. The results of this testing were analyzed to develop craze initiation criteria which apply to uniaxial and biaxial crazing.

2.2 THEORETICAL DEVELOPMENT OF CRAZE INITIATION

Craze initiation criterion are analogous to stress yielding criterion. Stress yielding criterion describe the necessary conditions (state of stress/strain) for yielding to occur. Stress yielding criterion which may apply to chemical stress crazing include:

maximum principal stress,
maximum principal strain,
maximum shear stress (Tresca),
distortional energy (von Mises),
strain energy, and
combinations of these, deviatoric stresses, and/or flow stresses.

These yielding criterion were considered as a starting point for the development of chemical stress crazing criterion.

While there is extensive information in the literature concerning stress yielding criterion (although most of it has not been applied specifically to polymers), there is limited information available in the literature concerning chemical stress crazing of polymers. The majority of the research which has been conducted has been concerned only with stress crazing, not chemical stress crazing. Two basic craze initiation criteria have been proposed. Sternstein and Ongchin (Reference 2) proposed a critical stress bias criterion for surface stress crazing of polymethylmethacrylate (PMMA, acrylic) as follows:

$$\sigma_1 - \sigma_2 \geq A/(\sigma_1 + \sigma_2) + B \qquad (1)$$

where σ_1 and σ_2 are the principle biaxial stresses, and A and B are functions of time and temperature. The difference between σ_1 and σ_2 represents a stress bias or flow stress (this is equal to twice the maximum shear stress), and the quantity of

$\sigma_1 + \sigma_2$ represents twice the first stress invariant or the mean stress. This criterion, along with the von Mises criterion for yielding (which has been shown by the same authors to be fairly representative of yielding behavior for acrylic) is plotted in biaxial stress space in Figure 2.1. Sternstein and Ongchin based their conclusions on cylindrical specimens under tension with internal pressure, and on combined tension/torsion tests, all at elevated temperatures (50°, 60°, and 70°C).

A second similar criterion, based on critical strain, has been developed by Oxborough and Bowden (Reference 3) for polystyrene, as follows:

$$\sigma_1 - \mu\sigma_2 = A/(\sigma_1 + \sigma_2) + B \qquad (2)$$

The only difference between this and the previous criterion is that the left side of the equation represents the maximum strain in this case, where μ is Poisson's ratio. Oxborough and Bowden based their conclusions on combined tensile and compressive tests, at room temperature, conducted on rectangular annealed polystyrene specimens with a hole in the center. This criterion plotted in stress space is similar to Figure 2.1.

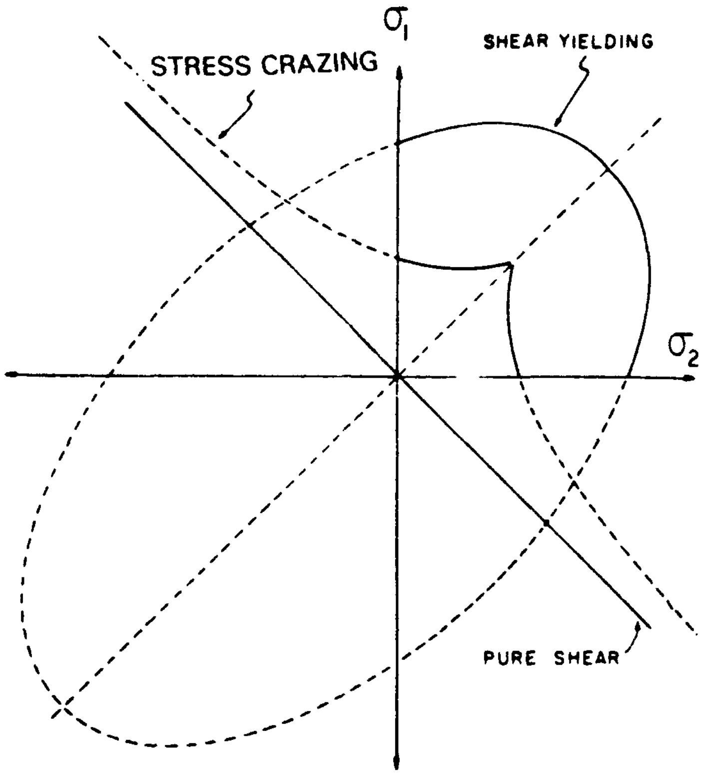

Figure 2.1. Biaxial Stress Yielding and Stress Crazing Curves for PMMA (from Ref. 2).

SECTION 3

CRAZE TESTING

3.1 UNIAXIAL CHEMICAL CRAZE TESTING

3.1.1 Specimen Configuration

The craze beam specimens were 1 inch x 7 inch x 1/8 inch thickness. Polycast Mil-P-8184 Type II (low moisture uptake) cast acrylic from the same lot was used for all testing.

3.1.2 Test Method

The craze beam testing was conducted using ASTM F484-83 as a guideline. The craze tests were conducted at 75 $\pm$ 10° F. The cantilever craze beams were loaded to produce a maximum stress at the fulcrum of 2000, 3000, and 4000 psi. The underside of the beams were marked at 0.25 inch intervals. After the load was applied, the beams were allowed to stabilize for ten minutes before the test chemical was applied to the beam surface. The edges of the beams were protected with a butyl rubber sealant to prevent the chemical from coming in contact with the machined or cut edges and causing premature crazing. Isopropyl alcohol (99% pure) was applied to the top surface of the beams as required to maintain a wetted condition. Time to craze initiation and location (corresponding to a discrete stress level) were recorded during the tests. The uniaxial chemical craze test setup is shown in Figure 3.1.

3.1.3 Test Data/Analysis

The results of the uniaxial craze tests are summarized in Figure 3.2. The uniaxial craze results plotted in Figure 3.2 indicate that there is a linear relationship between the log of time to initiation of craze and applied stress.

3.2 BIAXIAL CHEMICAL CRAZE TESTING

3.2.1 Specimen Configuration

The biaxial craze specimens were 8.5-inch diameter, 3/16-inch thick plate specimens. Polycast Mil-P-8184 Type II (low moisture uptake) cast acrylic from the same lot was again used for all testing.

3.2.2 Test Method

The craze tests were conducted using the general guidelines of ASTM F1164-88. The test fixturing included a pressure cell, a precision pressure regulator, and a pressure test gauge with accuracy of 0.075 psi. The test setup is shown

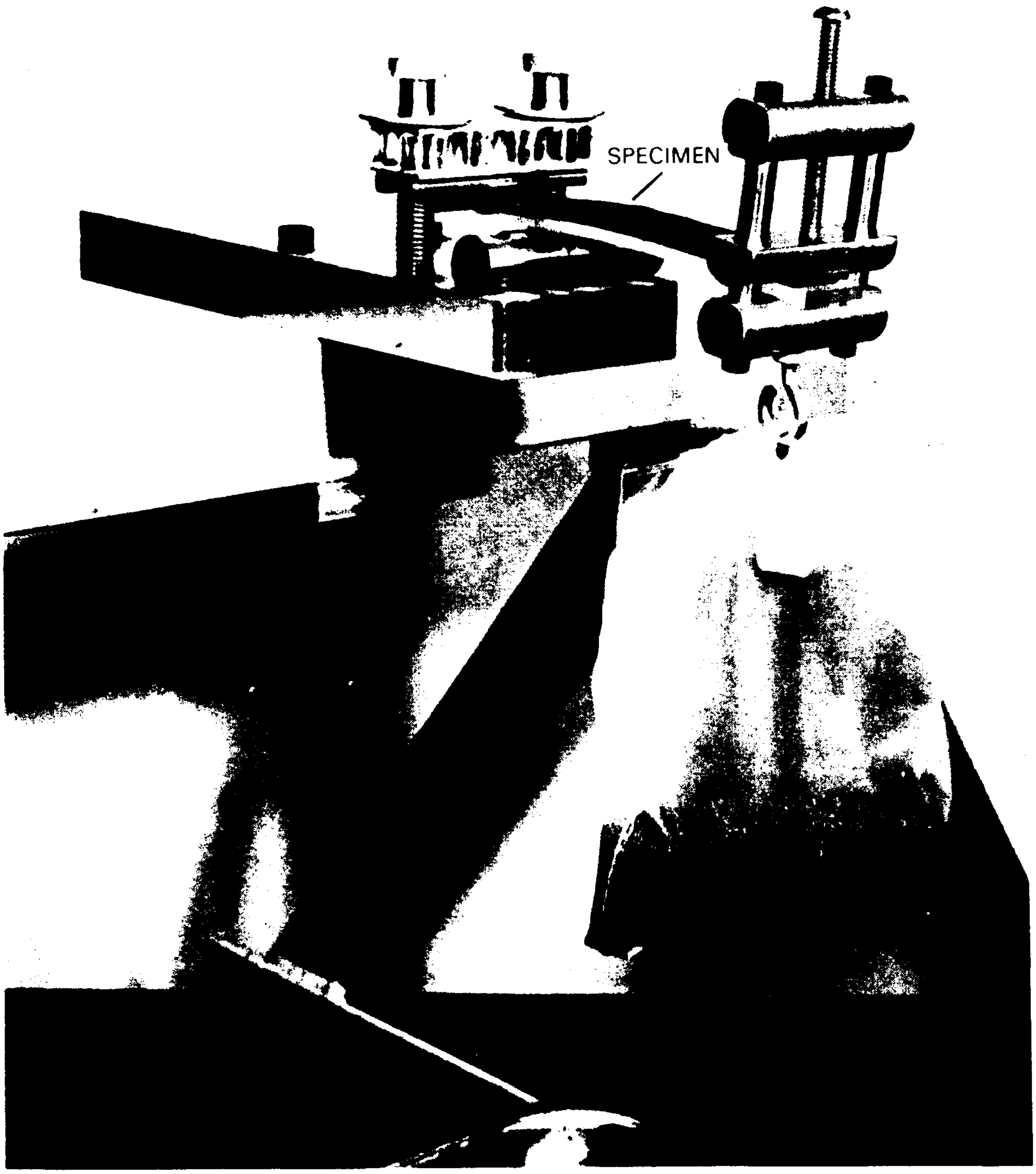

Figure 3.1. Uniaxial Chemical Craze Test Setup.

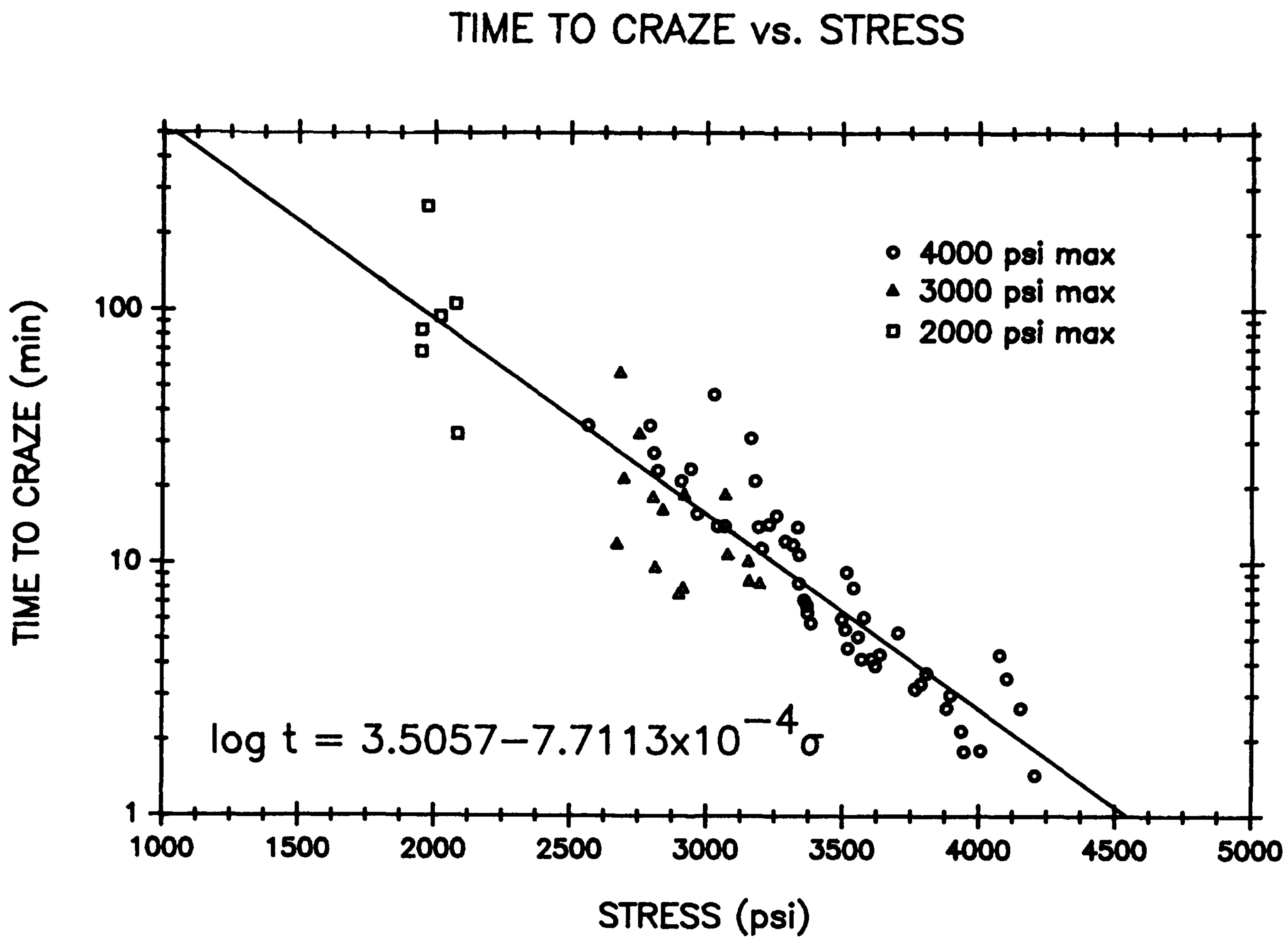

Figure 3.2. Uniaxial Craze Test Results.

in Figure 3.3. The pressure in the test cell was used to induce equal principal biaxial stresses of 2000, 3000, and 4000 psi at the center of the plates. Concentric rings were drawn on the underside of the plate to facilitate location of the crazes. The components of the principal stresses (the radial and tangential stresses) were determined from:

$$\sigma_r = \frac{3pR^2}{8t^2}\left[-(1+\mu) + (3+\mu)\frac{r^2}{R^2}\right] \tag{3}$$

$$\sigma_t = \frac{3pR^2}{8t^2}\left[-(1+\mu) + (1+3\mu)\frac{r^2}{R^2}\right] \tag{4}$$

where:

σ_r = radial stress (psi) σ_t = tangential stress (psi)

R = plate radius (inches) t = plate thickness (inches)

μ = Poisson's ratio p = pressure (psi)

r = radial dimension from center to point of interest (inches)

Figure 3.4 is a plot of the radial and tangential components of the stress in the biaxial plate specimen. After the pressure load was applied to the plate, the plates were allowed to stabilize for ten minutes before the test chemical was applied. Isopropyl alcohol (99% pure) was applied to the top surface of the plates as required to maintain a wetted condition. Time to craze initiation and location (corresponding to a discrete stress condition) were recorded during the tests.

3.2.3 Test Data/Analysis

The biaxial and uniaxial test data is presented in Figures 3.5-3.19. A typical tested biaxial specimen is shown in Figure 3.20. A biaxial craze specimen which was tested until failure is shown in Figure 3.21. It is believed that the spread in the data is due, in part, to the fact that each plot does not represent a discreet instant in time, but represents a time interval.

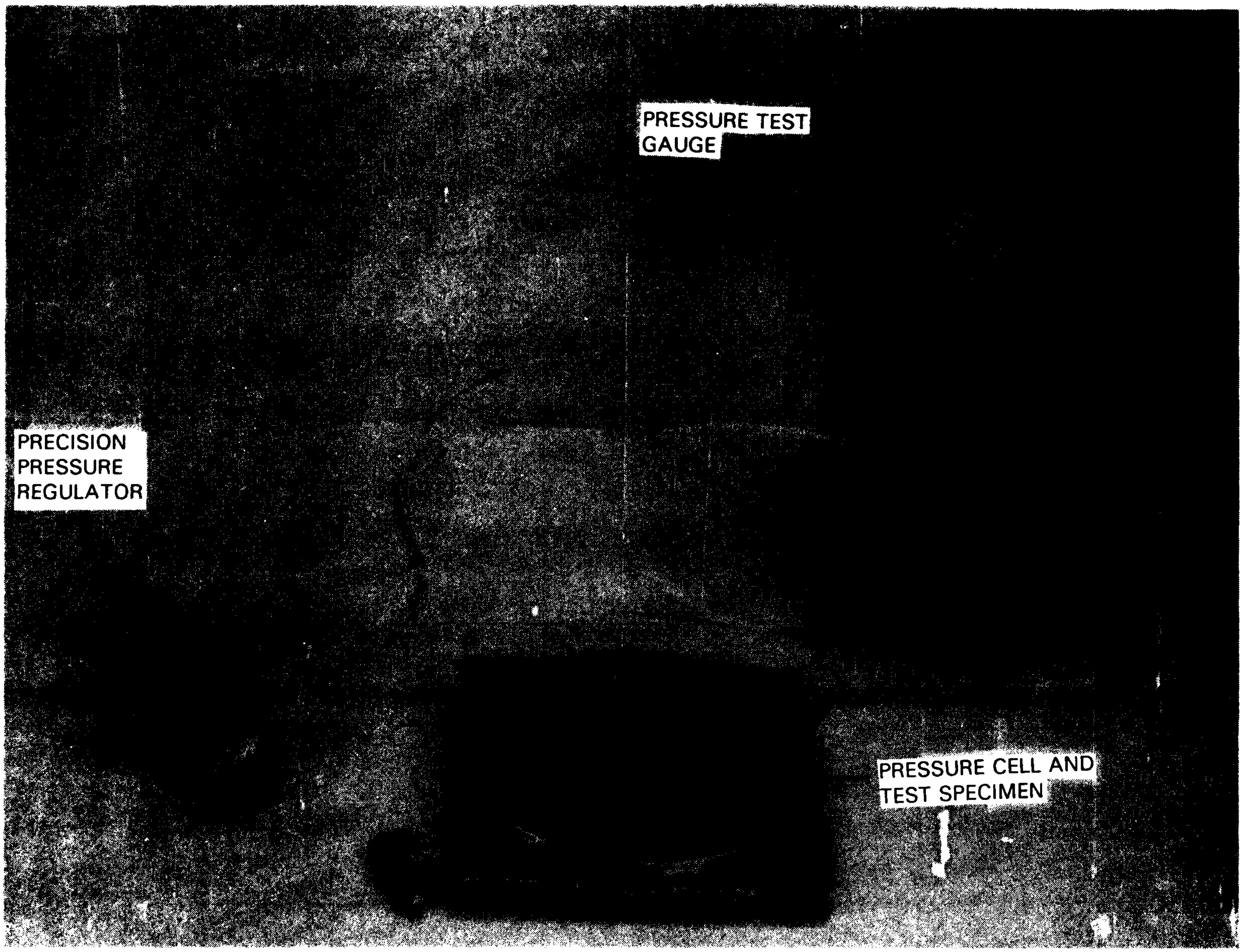

Figure 3.3. Biaxial Chemical Stress Craze Test Fixture.

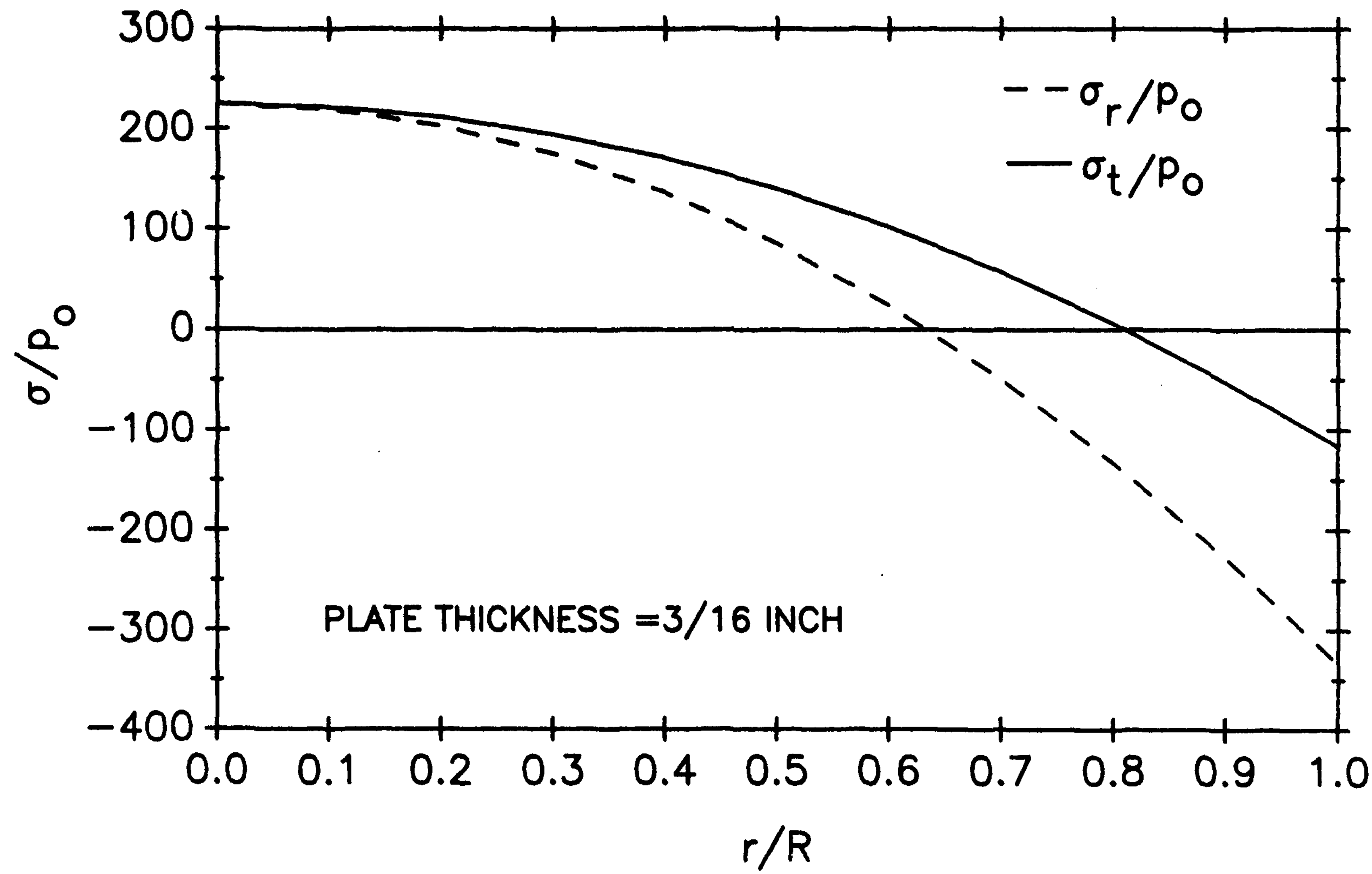

Figure 3.4. Radial and Tangential Components of the Stress in the Biaxial Plate Specimen.

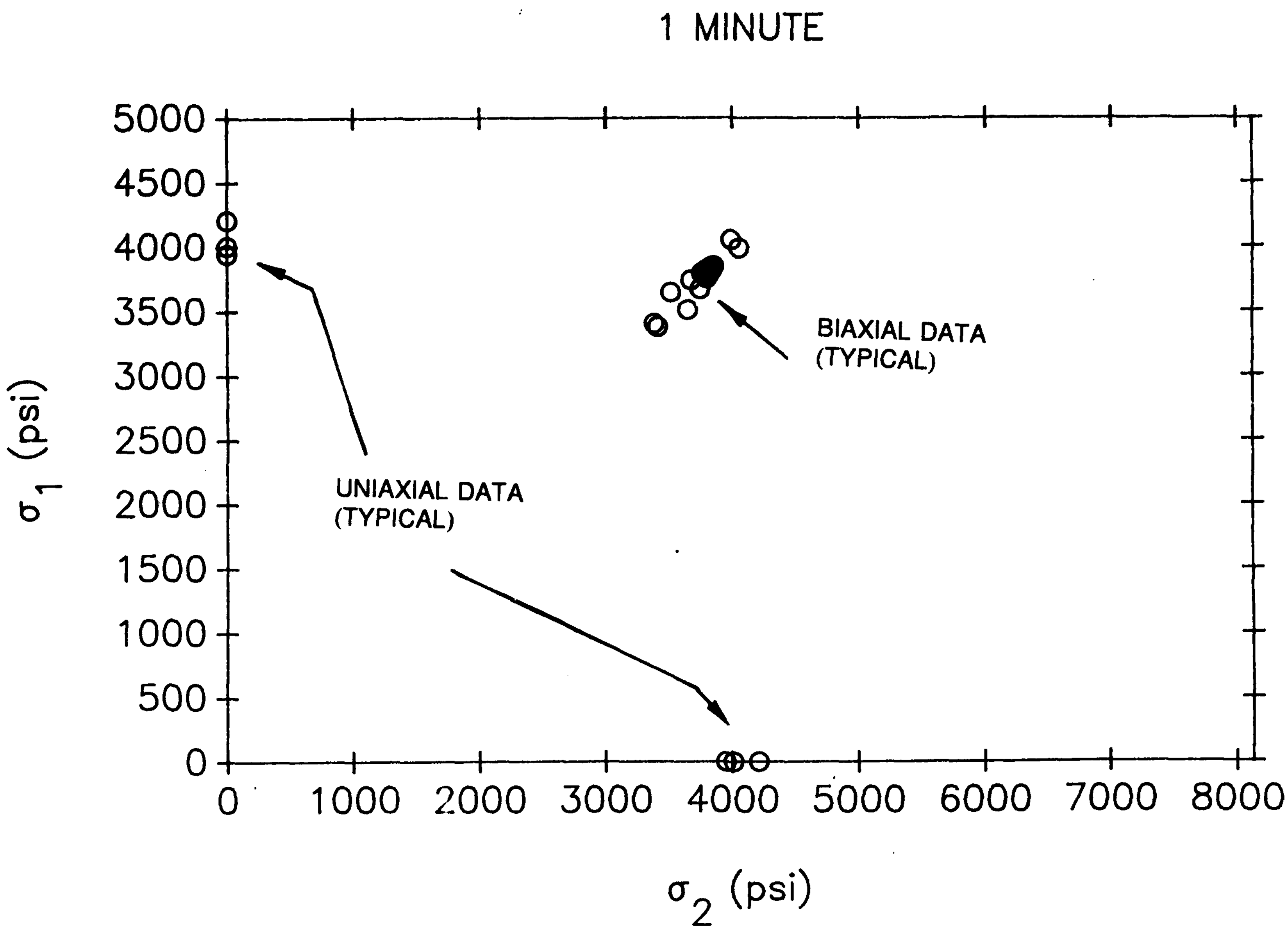

Figure 3.5. Plot of Uniaxial and Biaxial Chemical Craze Data at 1 Minute.

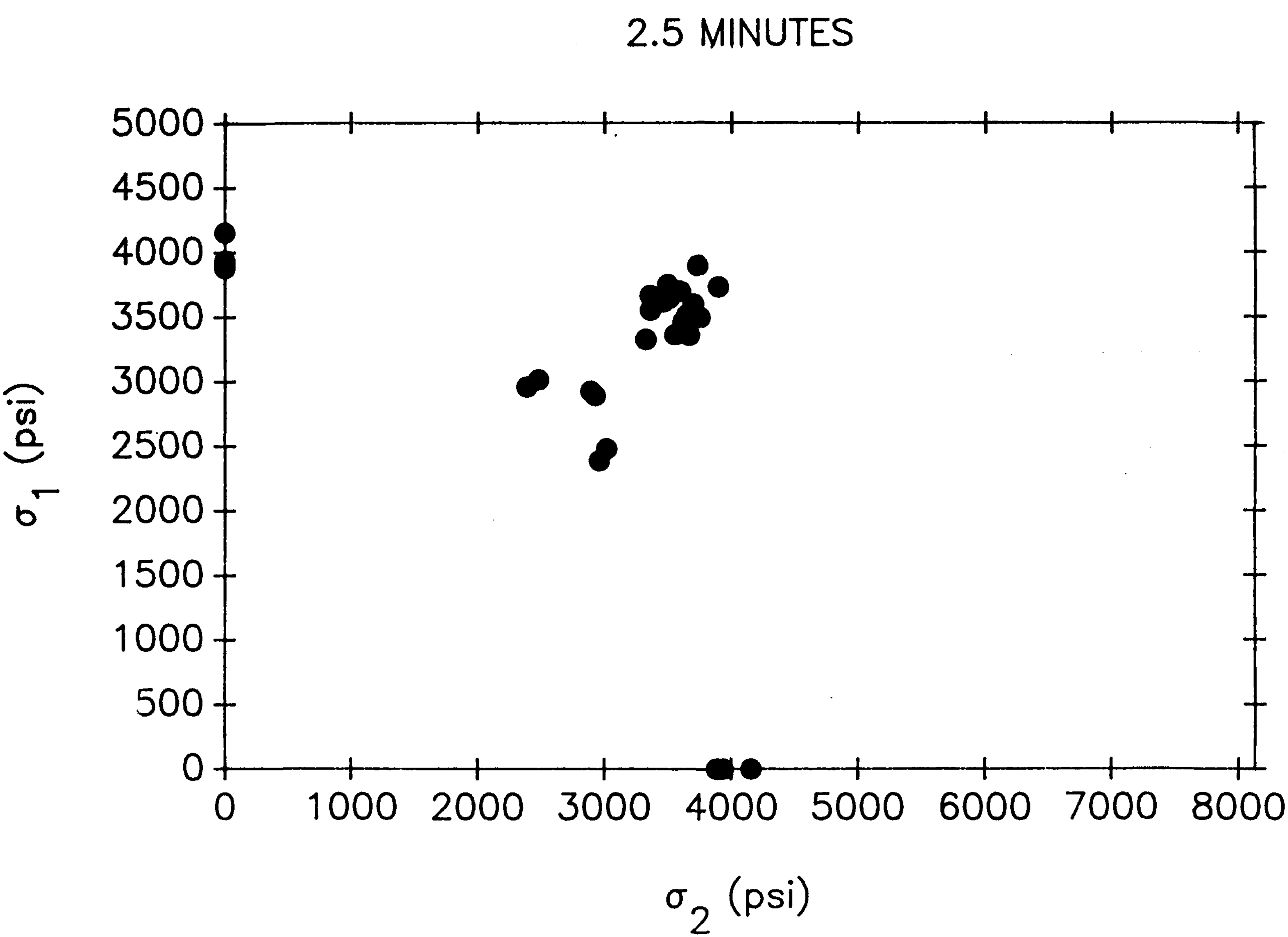

Figure 3.6. Plot of Uniaxial and Biaxial Chemical Craze Data at 2.5 Minutes.

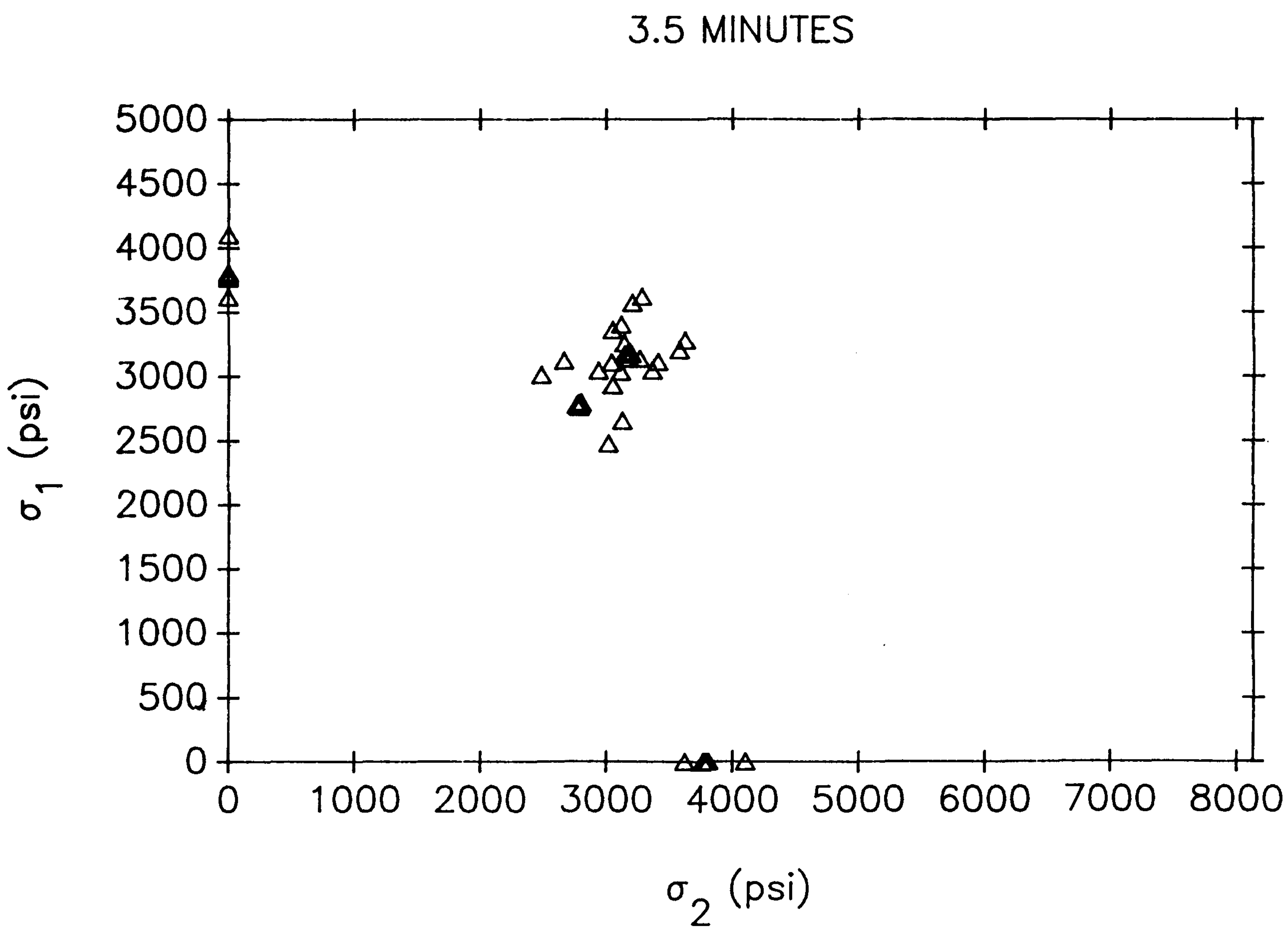

Figure 3.7. Plot of Uniaxial and Biaxial Chemical Craze Data at 3.5 Minutes.

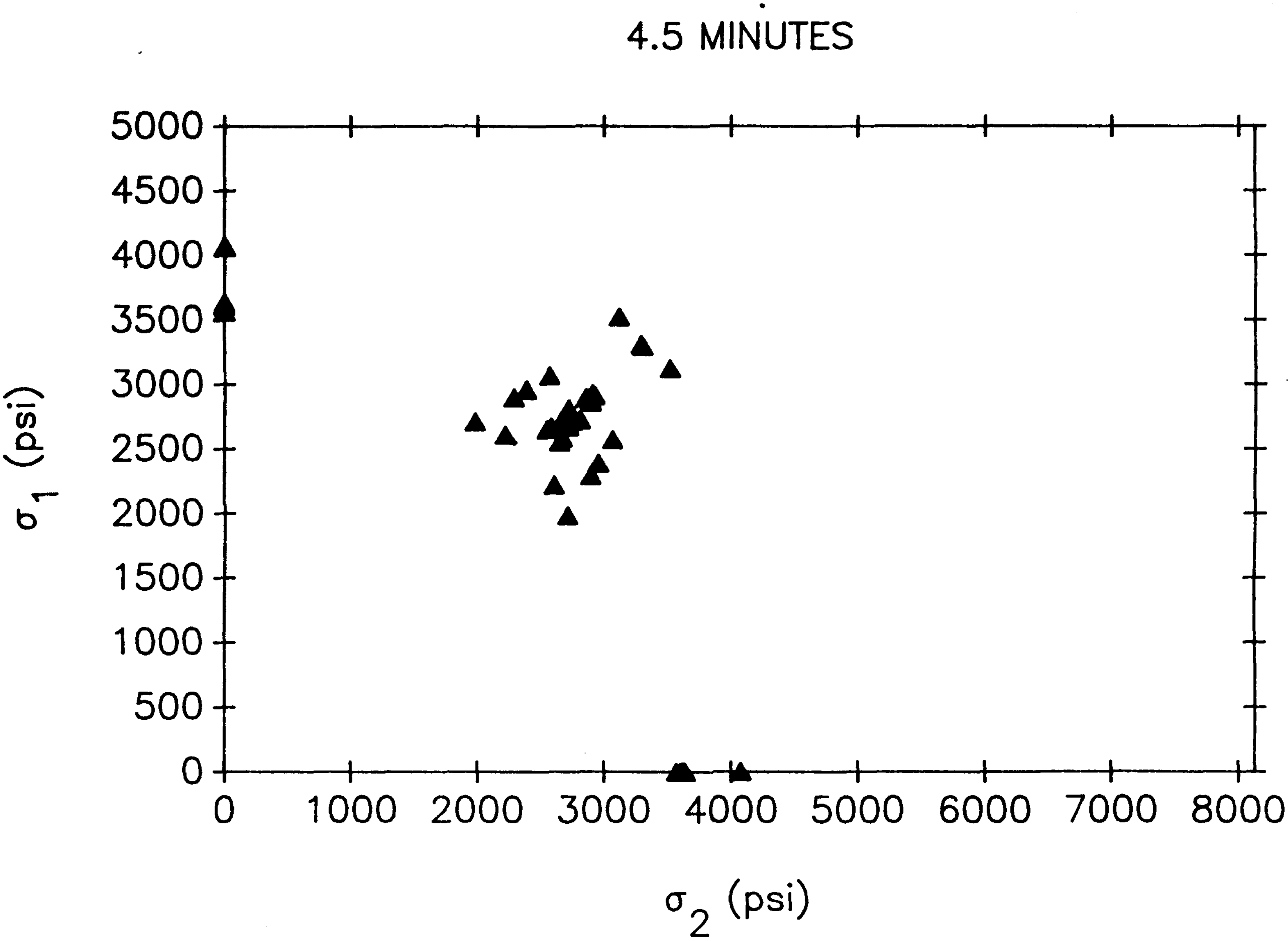

Figure 3.8. Plot of Uniaxial and Biaxial Chemical Craze Data at 4.5 Minutes.

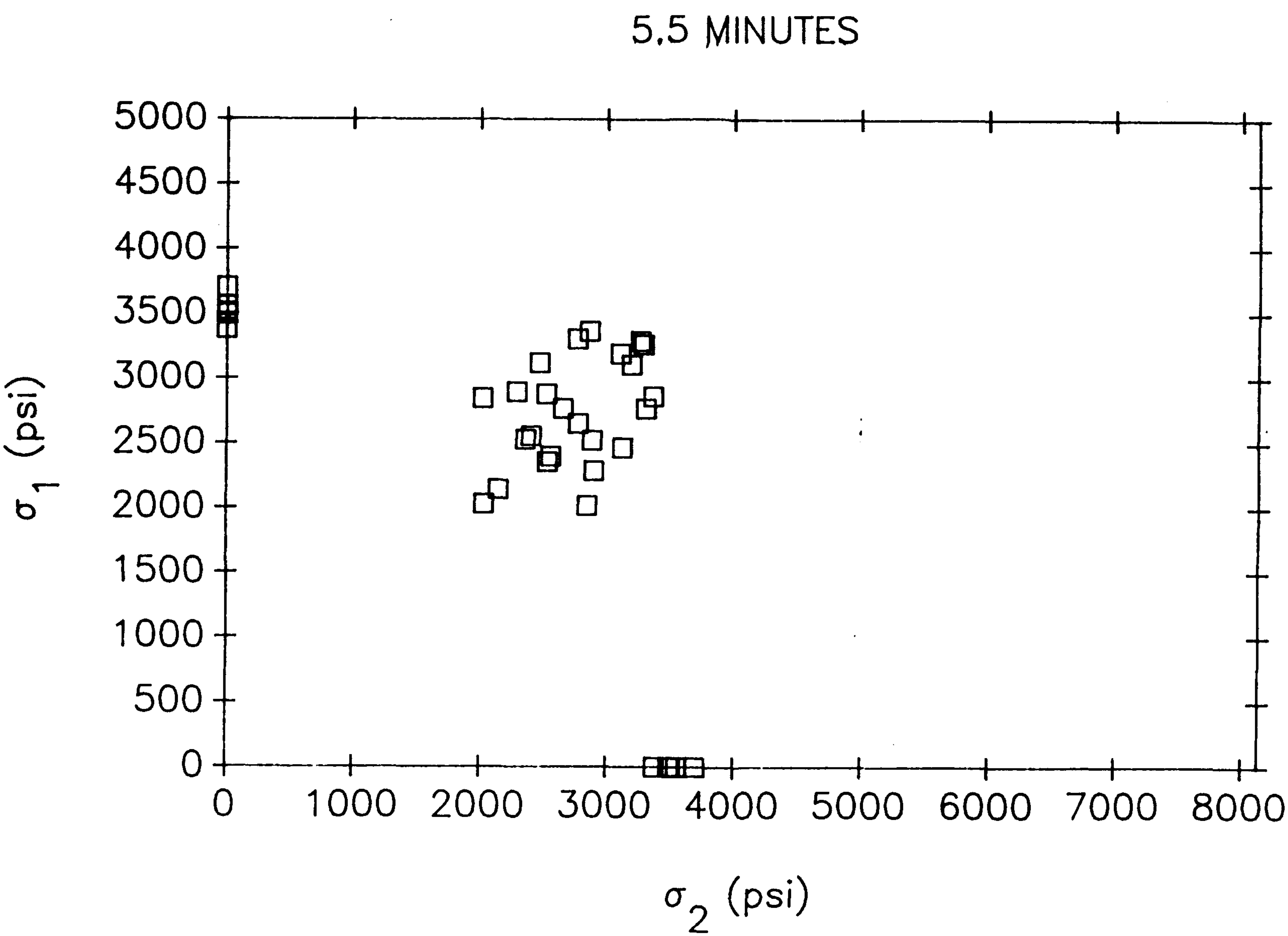

Figure 3.9. Plot of Uniaxial and Biaxial Chemical Craze Data at 5.5 Minutes.

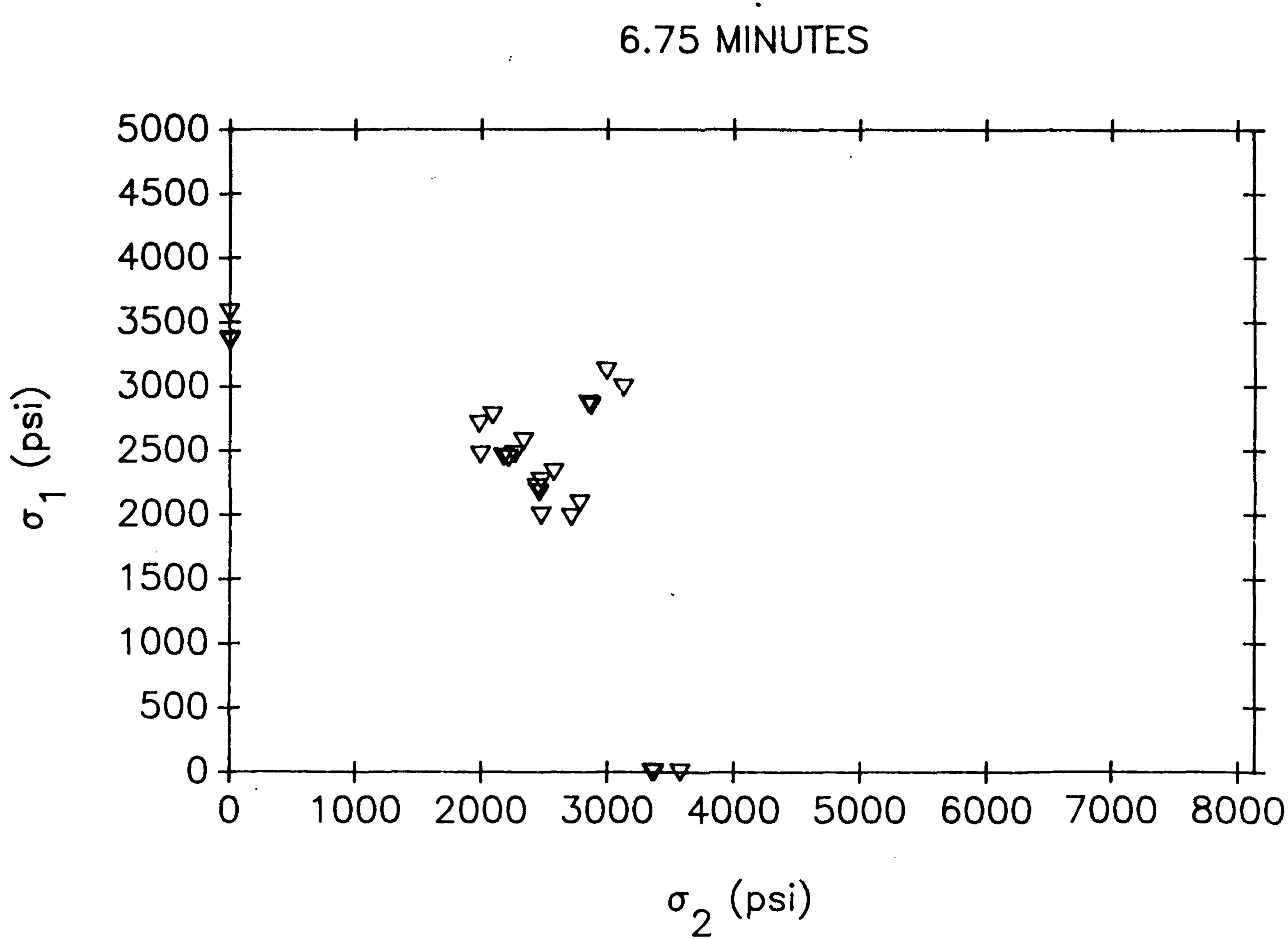

Figure 3.10. Plot of Uniaxial and Biaxial Chemical Craze Data at 6.75 Minutes.

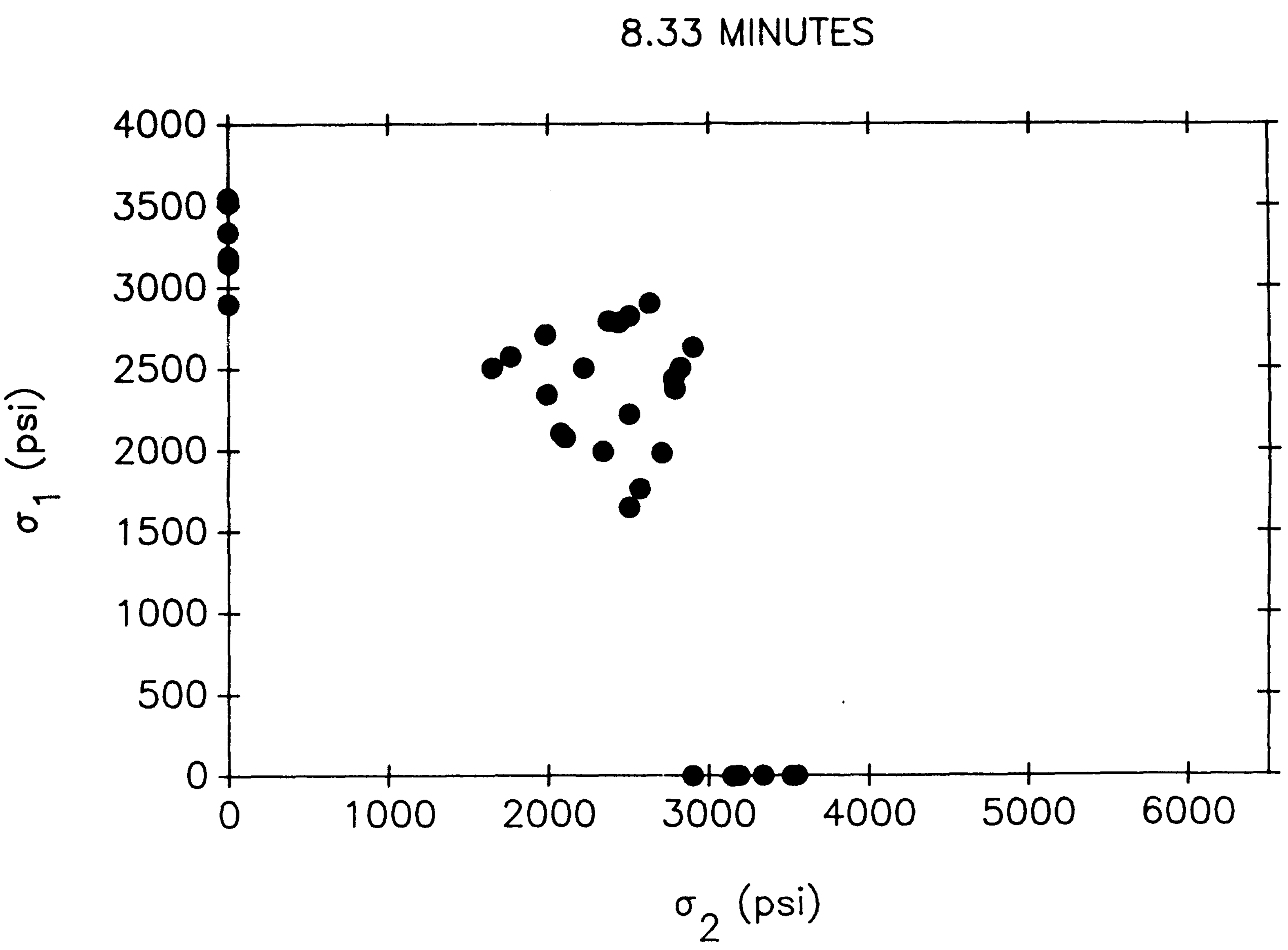

Figure 3.11. Plot of Uniaxial and Biaxial Chemical Craze Data at 8.33 Minutes.

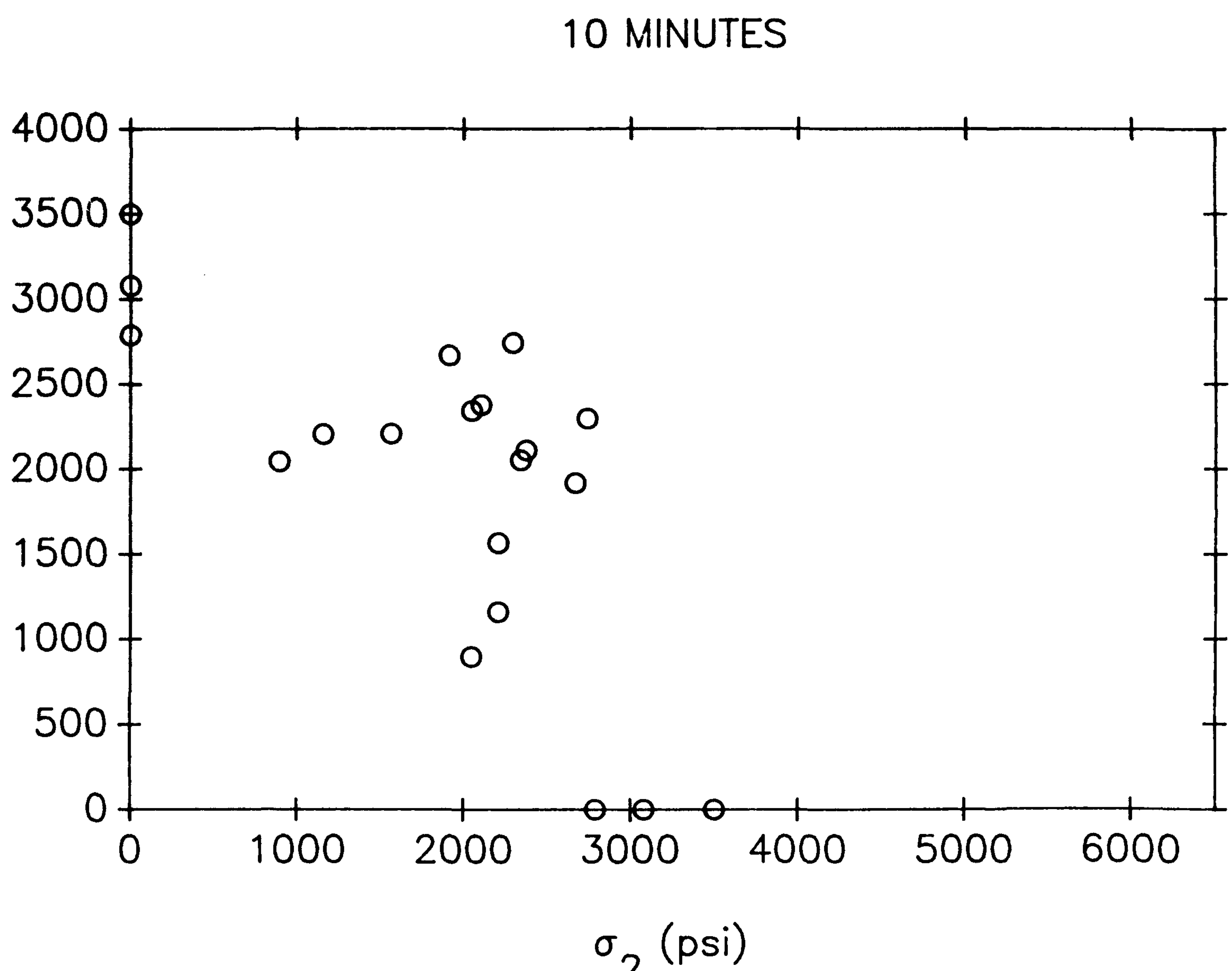

Figure 3.12. Plot of Uniaxial and Biaxial Chemical Craze Data at 10 Minutes.

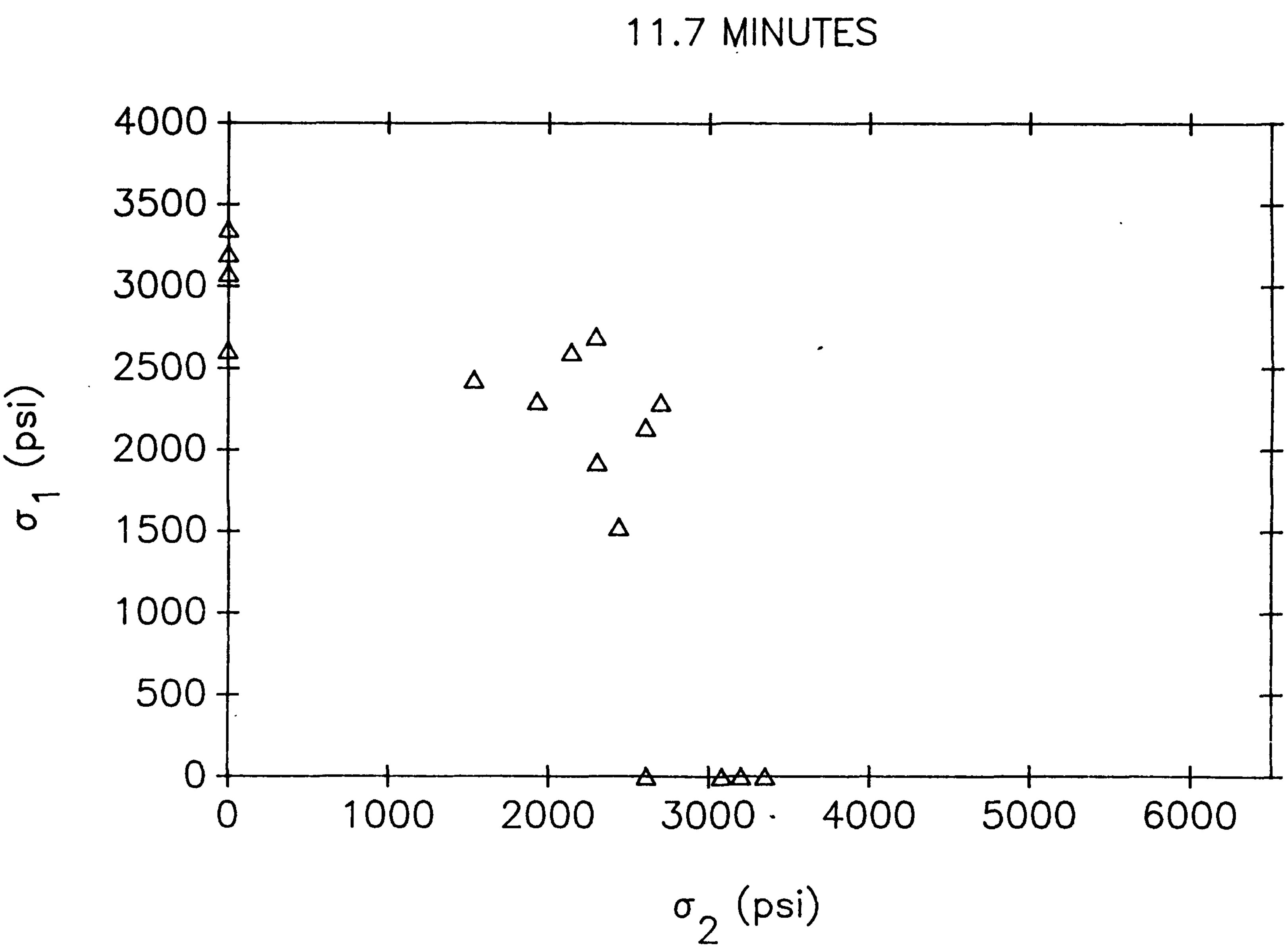

Figure 3.13. Plot of Uniaxial and Biaxial Chemical Craze Data at 11.7 Minutes.

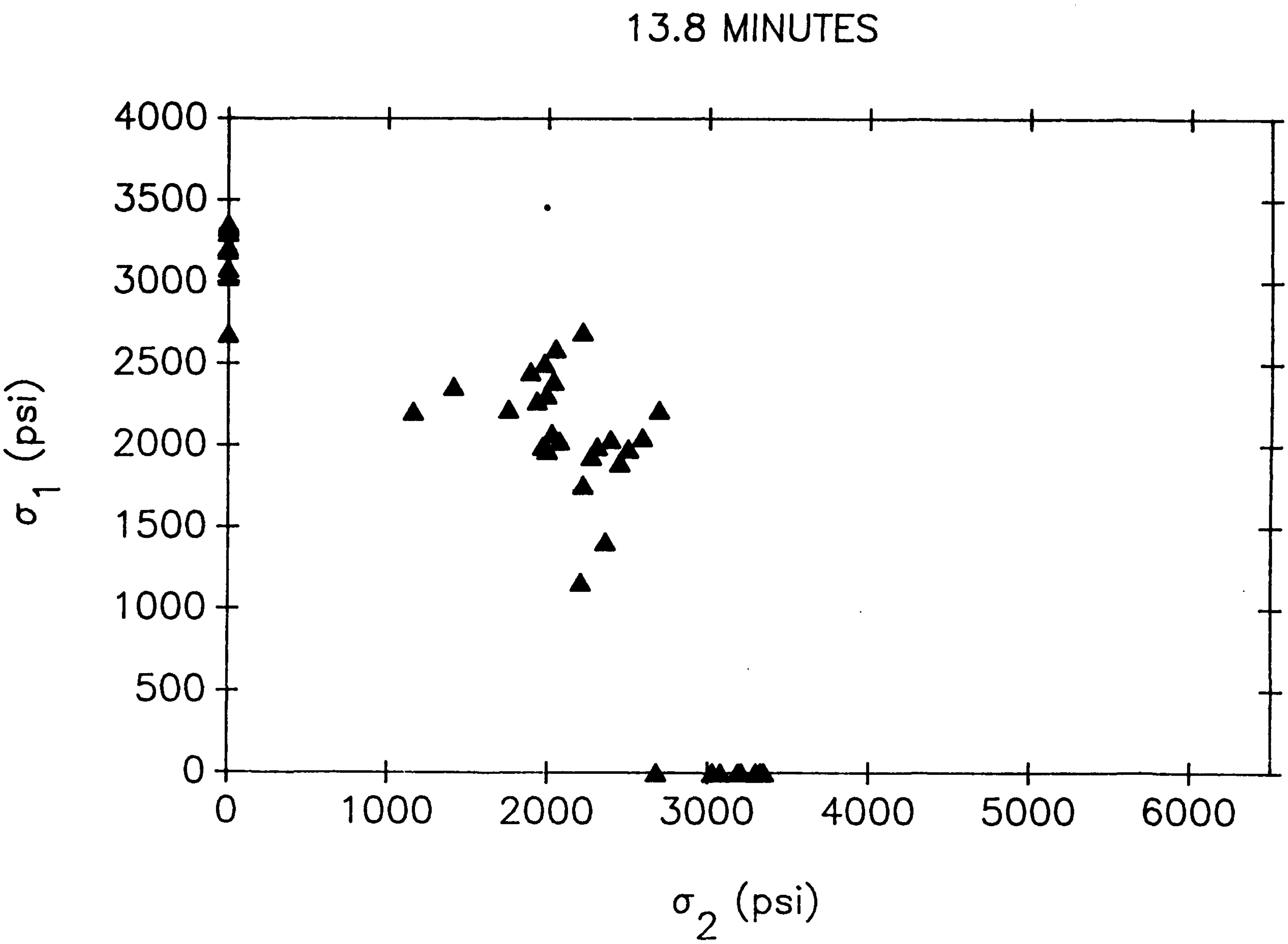

Figure 3.14. Plot of Uniaxial and Biaxial Chemical Craze Data at 13.8 Minutes.

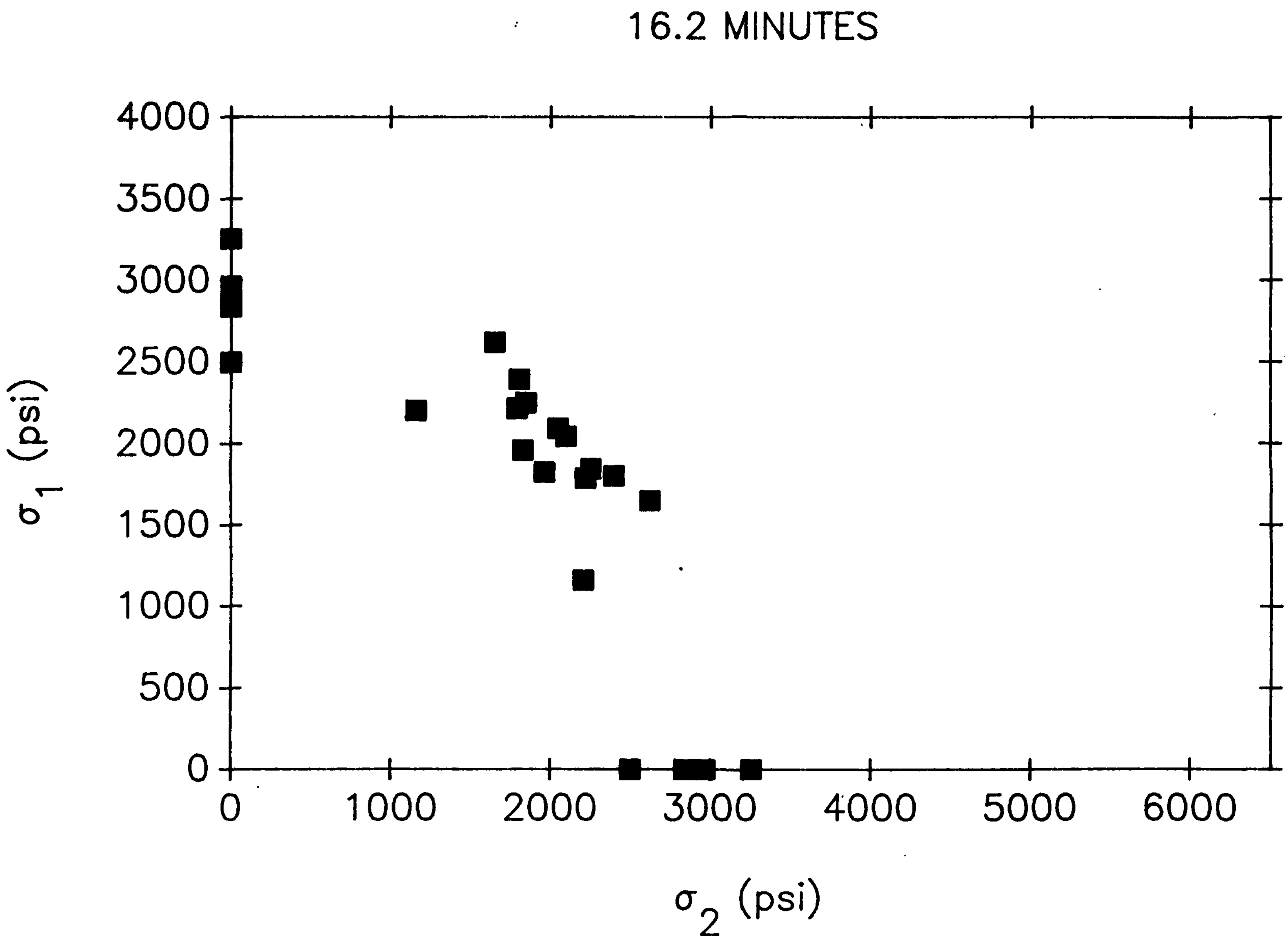

Figure 3.15. Plot of Uniaxial and Biaxial Chemical Craze Data at 16.2 Minutes.

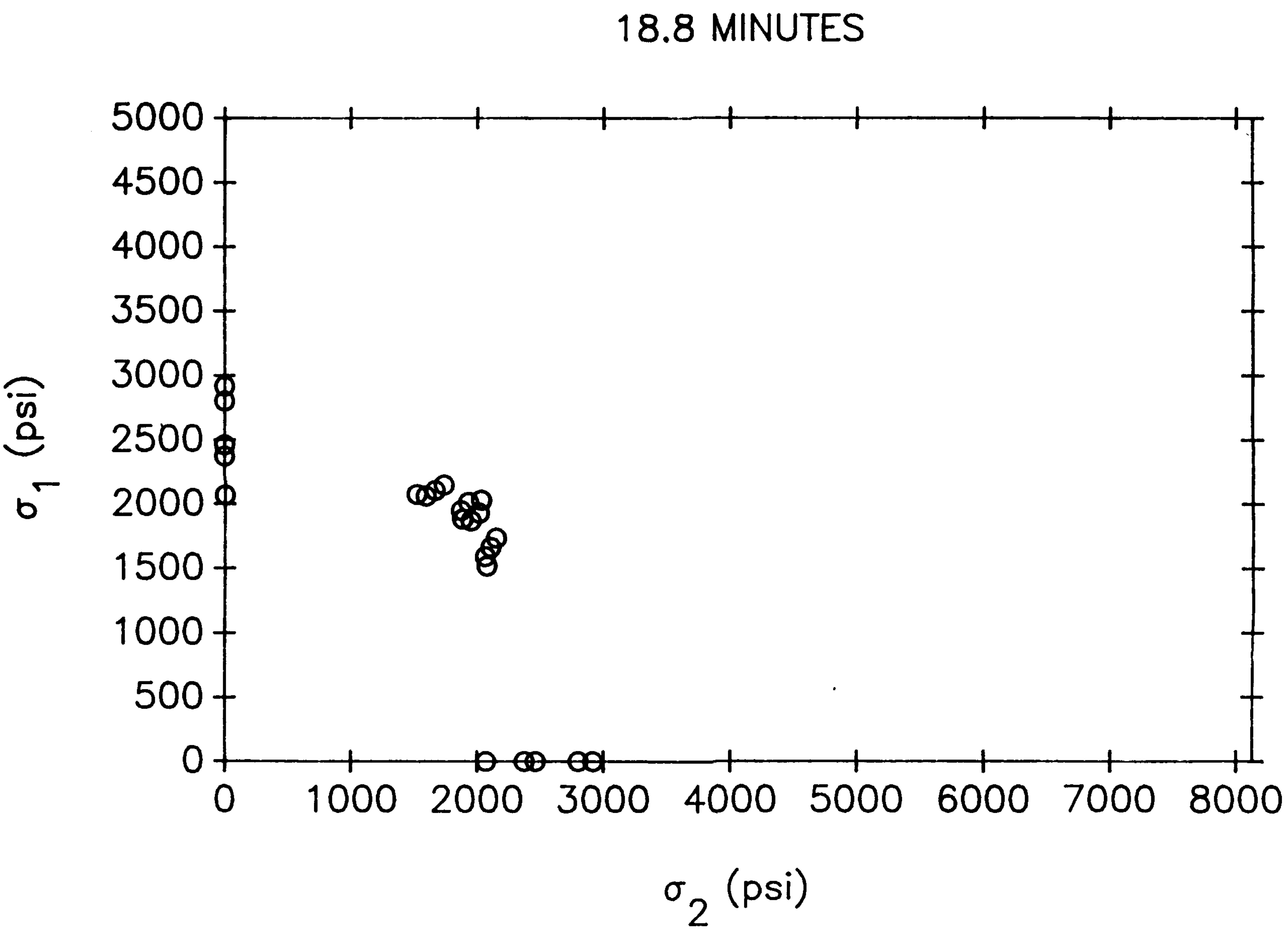

Figure 3.16. Plot of Uniaxial and Biaxial Chemical Craze Data at 18.8 Minutes.

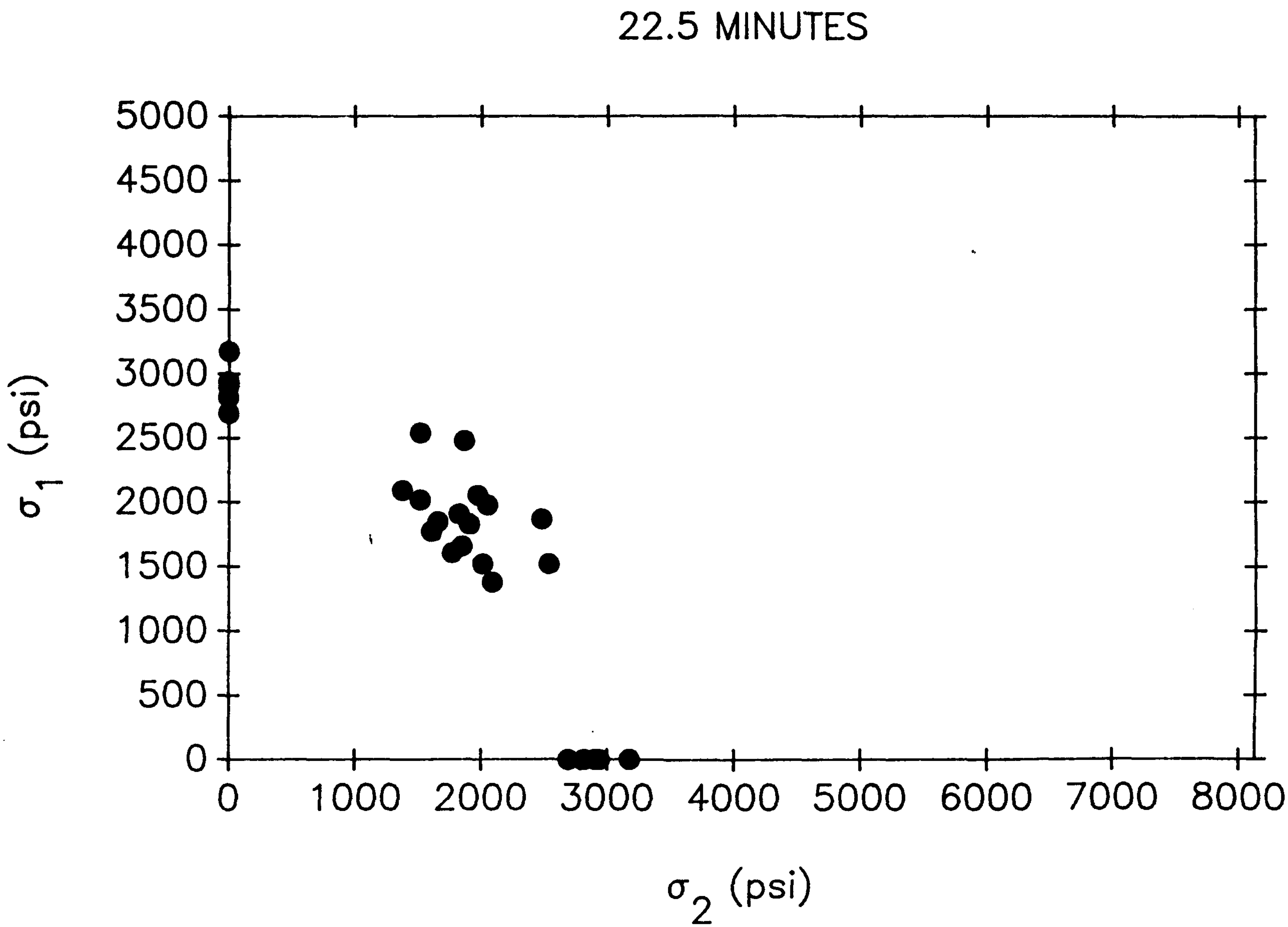

Figure 3.17. Plot of Uniaxial and Biaxial Chemical Craze Data at 22.5 Minutes.

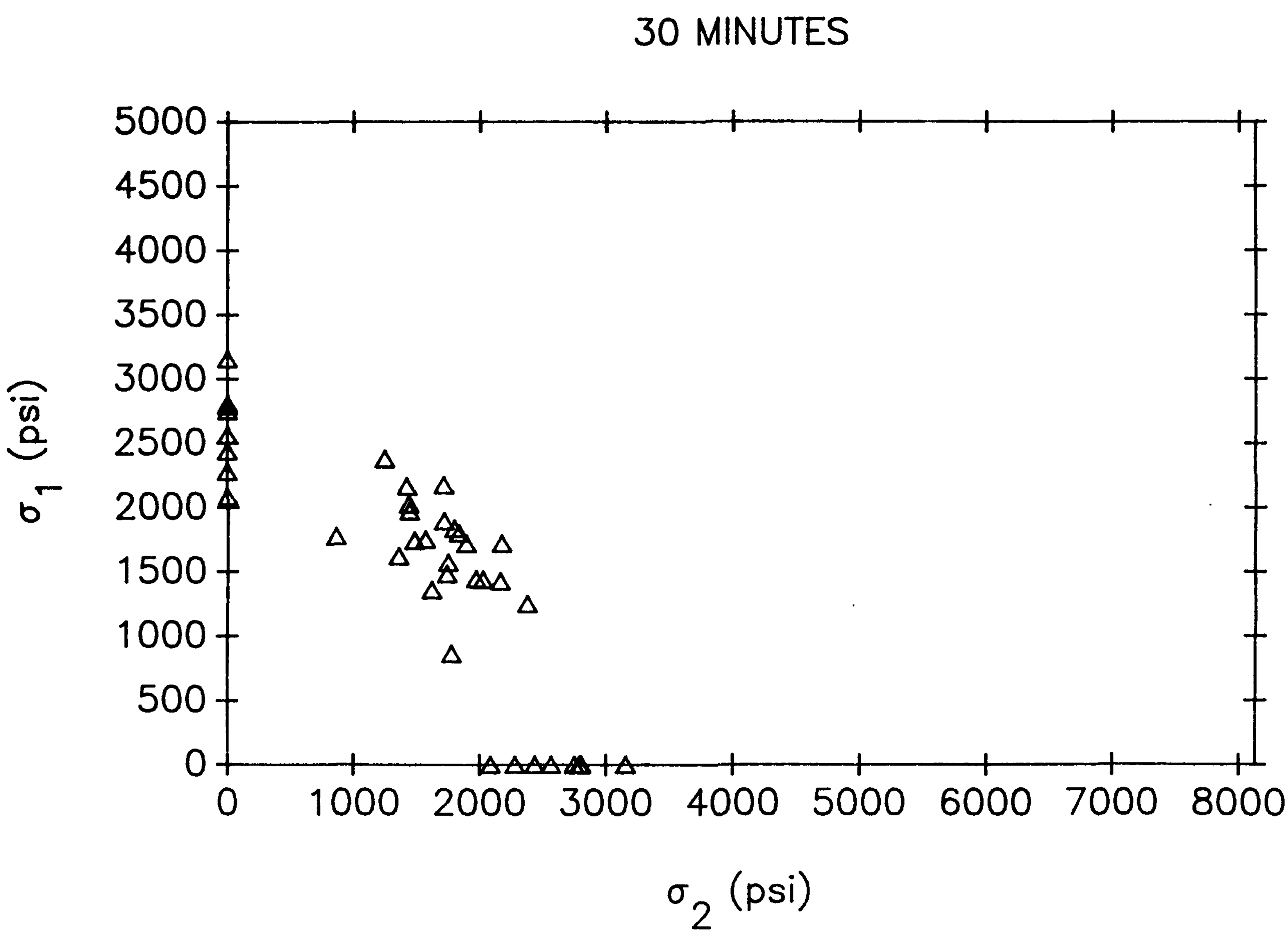

Figure 3.18. Plot of Uniaxial and Biaxial Chemical Craze Data at 30 Minutes.

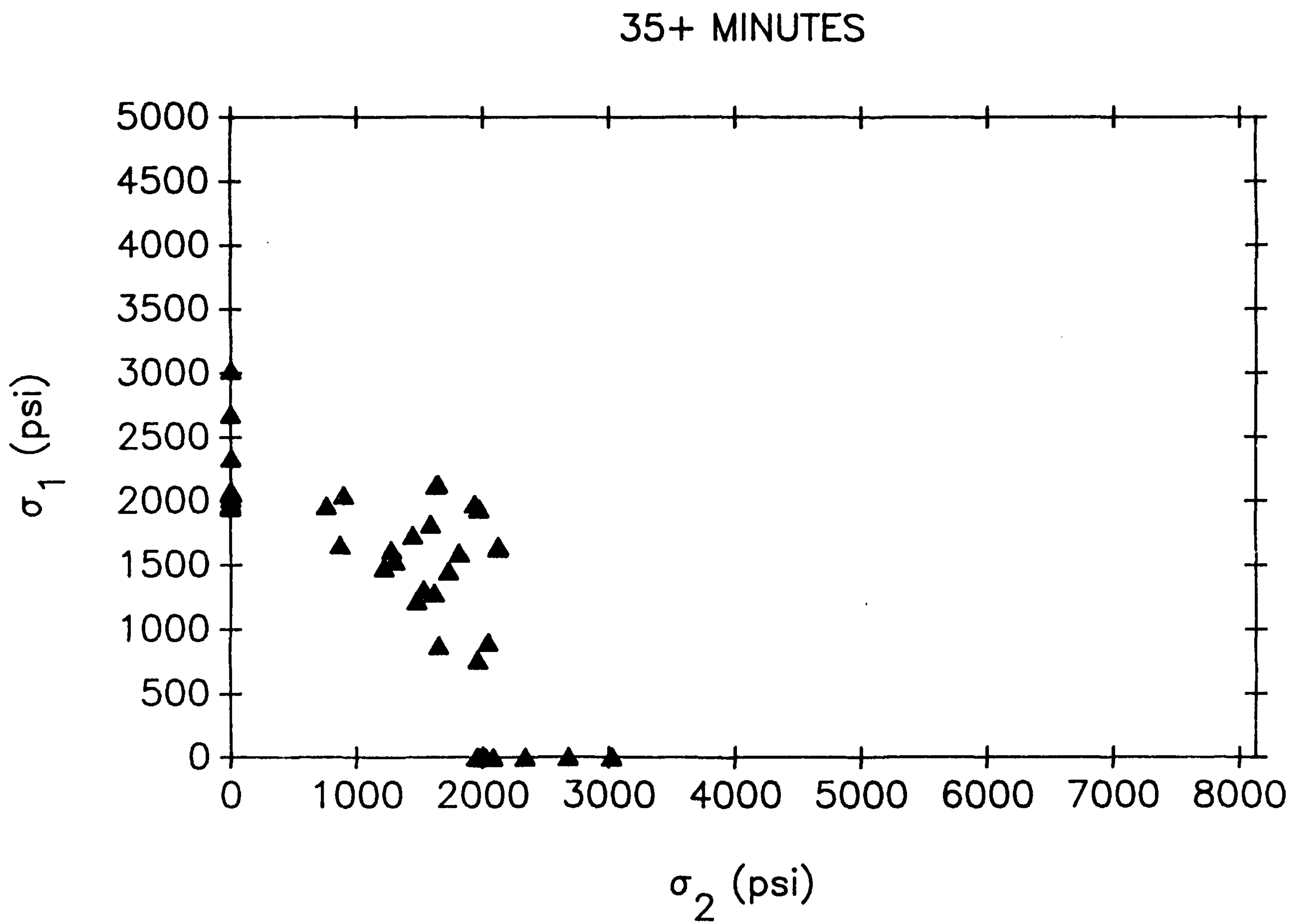

Figure 3.19. Plot of Uniaxial and Biaxial Chemical Craze Data at 35+ Minutes.

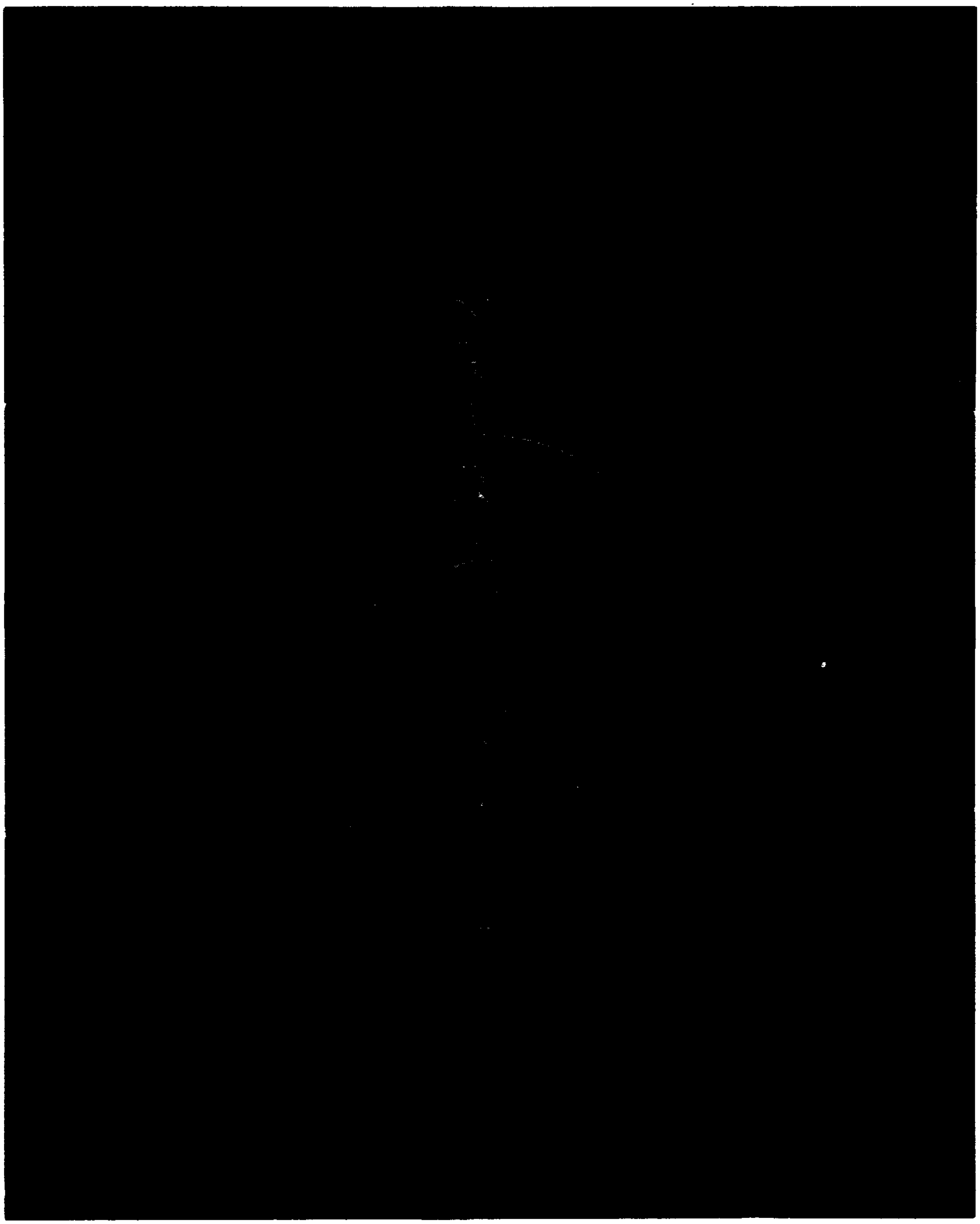

Figure 3.20. Typical Tested Biaxial Craze Specimen.

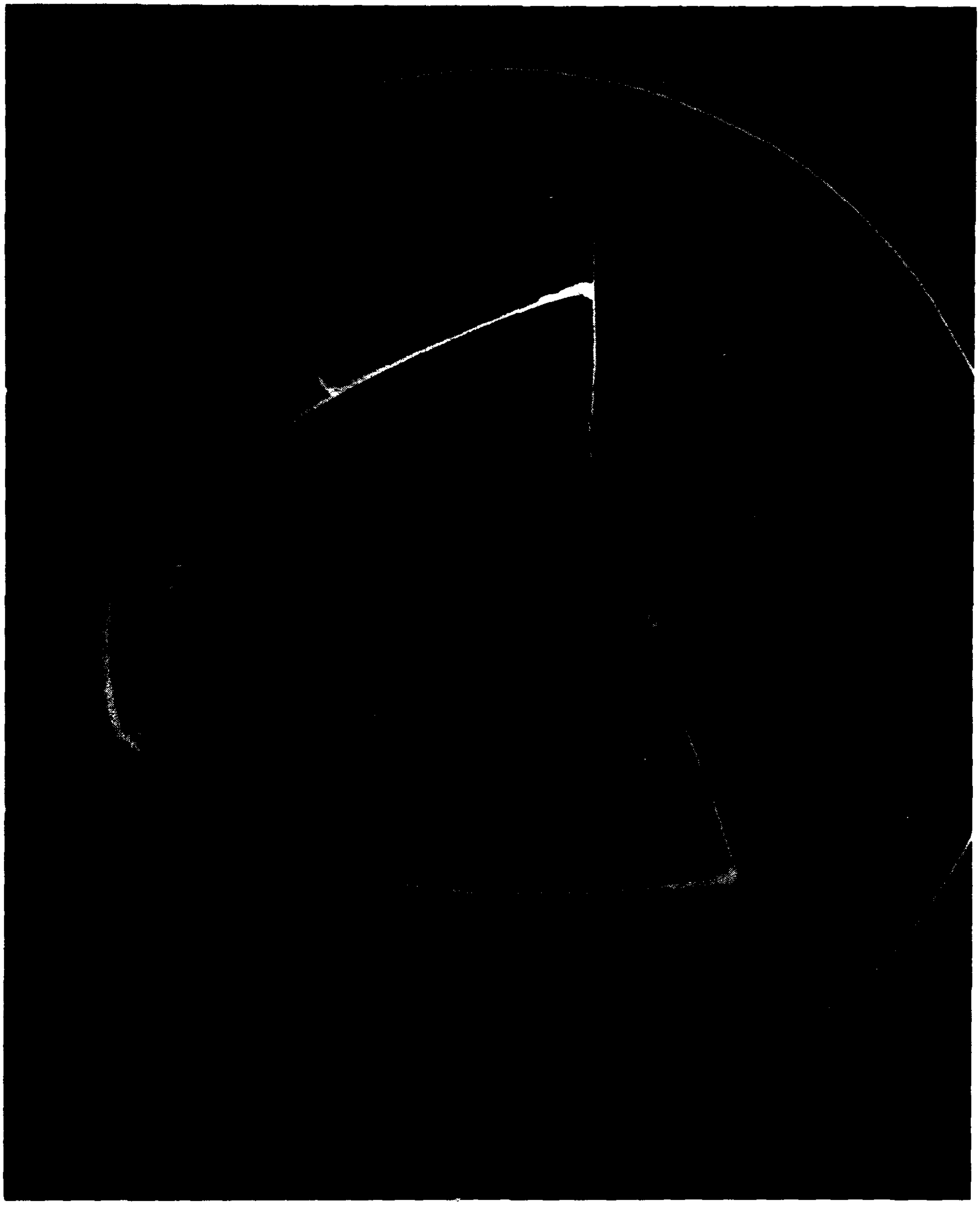

Figure 3.21. Biaxial Craze Specimen Tested to Failure.

SECTION 4

EVALUATION OF CRAZE INITIATION CRITERION

All of the types of yield initiation criterion listed in Section 2 were evaluated. None of these criterion fit the data in the forms that they have been used to describe yielding. The elliptical shape of the von Mises and strain energy criterion showed promise, but did not fit the uniaxial and biaxial data generated by test.

Equations 1 and 2, which are semi-empirical, were also evaluated. Because of the limitations of biaxial stress combinations which can be obtained from the biaxial plate specimens (the biaxial plate is only effective for measuring tensile-tensile stress loads of limited combinations; see Figure 3.4), it is difficult to determine if the shape of the craze initiation surface in stress space is cusp shaped as shown in Figure 2.1, or if it is some other shape.

The parameters A and B from equations 1 and 2 were determined as follows:

For the uniaxial stress state, Equation 1 (stress bias criterion) reduces to

$$\sigma = A/\sigma + B \tag{5}$$

A least square fit of the data in Figure 3.2 provides a relationship between time to craze and uniaxial stress

$$\log t = 3.5057 - 7.7113\text{x}10^{-4}\sigma \tag{6}$$

or, rearranging to solve for stress in terms of time,

$$\sigma = (3.5057 - \log t)/(7.7113 \times 10^{-4}) \tag{7}$$

Substituting Equation 5 into Equation 3, and solving for B,

$$\begin{aligned} B = {} & (3.5057 - \log t)/(7.7113 \times 10^{-4}) \\ & - A/(3.5057 - \log t)/(7.7113 \times 10^{-4}) \end{aligned} \tag{8}$$

Equation 8 is then substituted into Equation 1, leaving A, σ_1, and σ_2 as the only unknowns.

$$\sigma_1 - \sigma_2 \geq A/(\sigma_1 + \sigma_2) + (3.5057 - \log t)/(7.7113 \times 10^{-4}) - A/(3.5057 - \log t)/(7.7113 \times 10^{-4}) \qquad (9)$$

Equation 9 is then rearranged to solve for A, and the biaxial test data is then input into the equation to determine A for each test data set σ_1, σ_2, and time t. The corresponding value for B is determined from Equation 8. The values of A and B are then plotted versus time, see Figures 4.1 and 4.2, and a least square fit provides a relationship between the value A and time, and the value B and time. Note that the coefficients of determination, R, for A and B are shown on Figures 4.1 and 4.2. The coefficient of determination, R, is a measure of the standard error associated with the least square fit to the data. Possible values range from 0 to 1. The closer the R value is to 1, the smaller the standard error is for the straight line fit to the data. Equation 1 (stress bias criterion) plotted in the first quadrant of stress space (tension-tension) with the functions for A and B shown in Figures 4.1 and 4.2, is shown in Figure 4.3.

The parameters A and B for Equation 2 (maximum strain criterion) are solved for in a similar manner and, along with corresponding R values, are shown in Figures 4.4 and 4.5. Equation 2 (maximum strain criterion), plotted in the first quadrant of stress space with the functions for A and B shown in Figures 4.4 and 4.5, is shown in Figure 4.6.

Most accepted yield criterion are elliptical in shape (e.g., von Mises and strain energy). In fact, the plots of biaxial and uniaxial results for the later time periods (after 15 minutes) appear to be elliptical shaped. The general formula for an ellipse oriented at 45° to the x and y axis is

$$(\sigma_1^2 + 2\sigma_1\sigma_2 + \sigma_2^2)/A^2 + (\sigma_1^2 - 2\sigma_1\sigma_2 + \sigma_2^2)/B^2 = 2 \qquad (10)$$

where the parameters A and B are functions of time. A and B are solved for in a manner similar to that shown above. The parameters A and B are plotted versus time in Figures 4.7 and 4.8. A family of empirical elliptical shaped craze initiation criteria curves, plotted using Equation 10 and the equations for A and B shown in Figures 4.7 and 4.8, are shown in Figure 4.9. A plot of this craze initiation criteria in biaxial stress and time space is shown in Figure 4.10. This surface represents the threshold between uncrazed and crazed material. Inside the surface there is not sufficient energy to cause crazing. The craze surface (and condition) can be reached by increasing the available energy; the available energy is increased by moving up the time scale, increasing the stresses, and/or increasing the temperature.

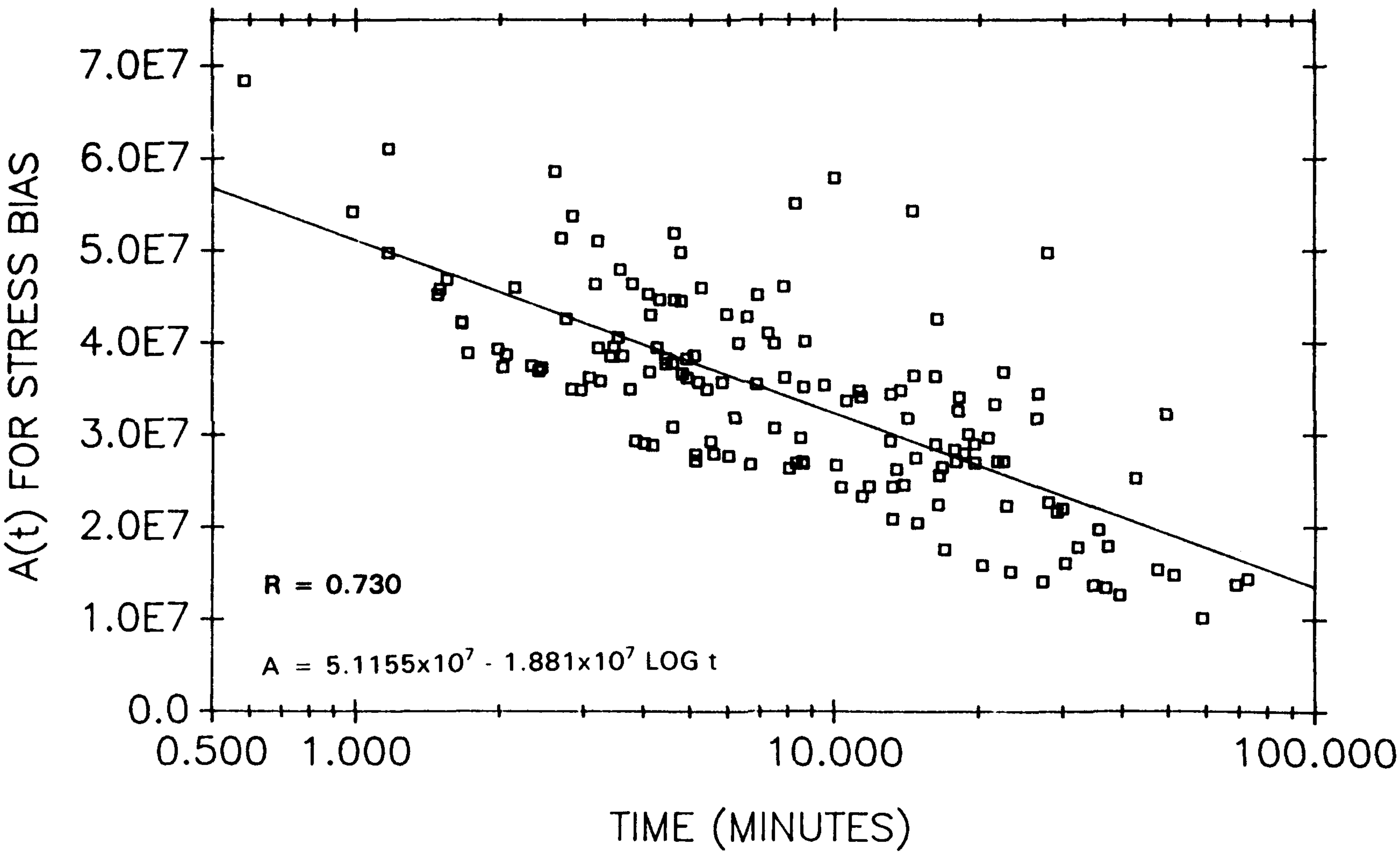

Figure 4.1. Parameter A as a Function of Time for Stress Bias Criteria.

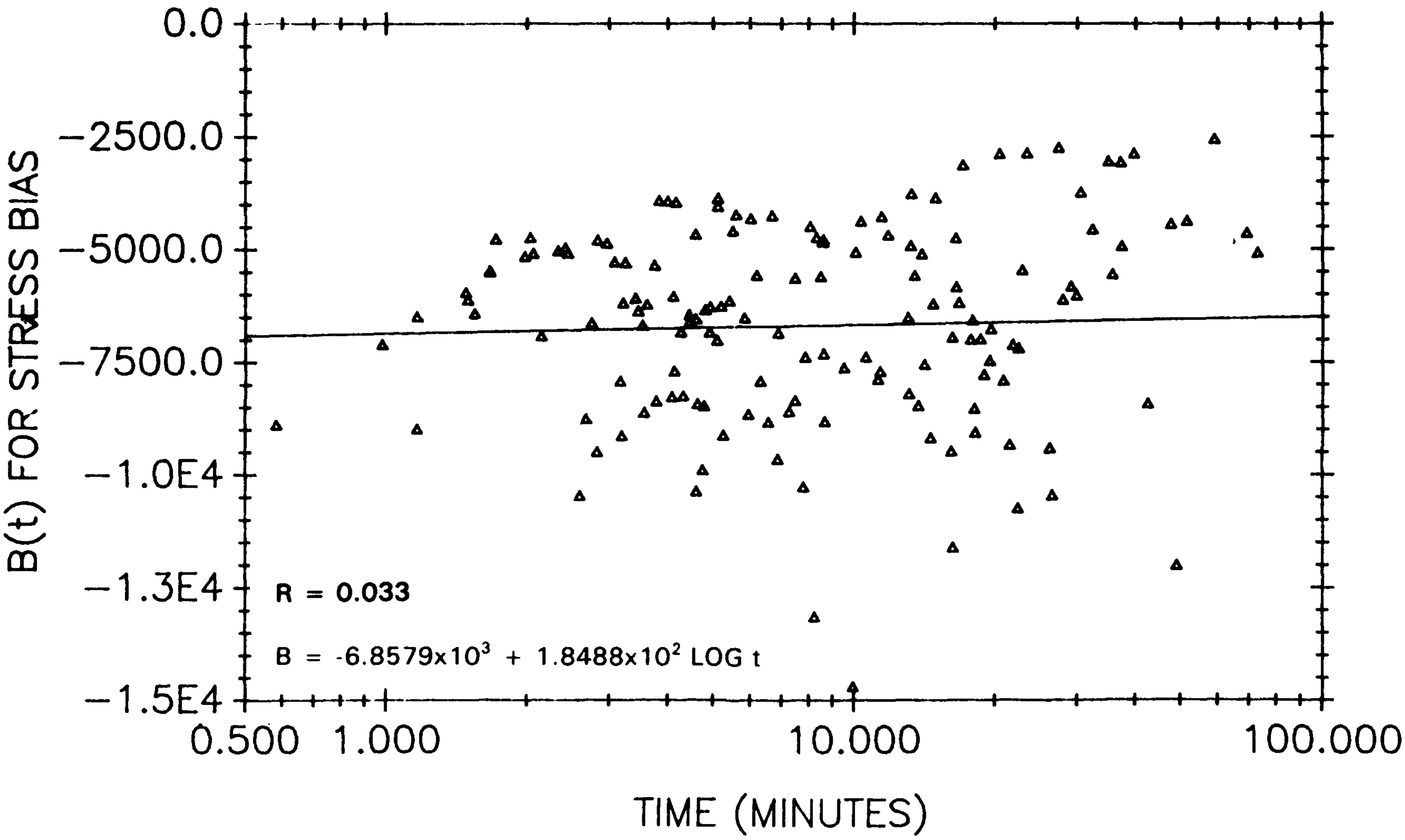

Figure 4.2. Parameter B as a Function of Time for Stress Bias Criteria.

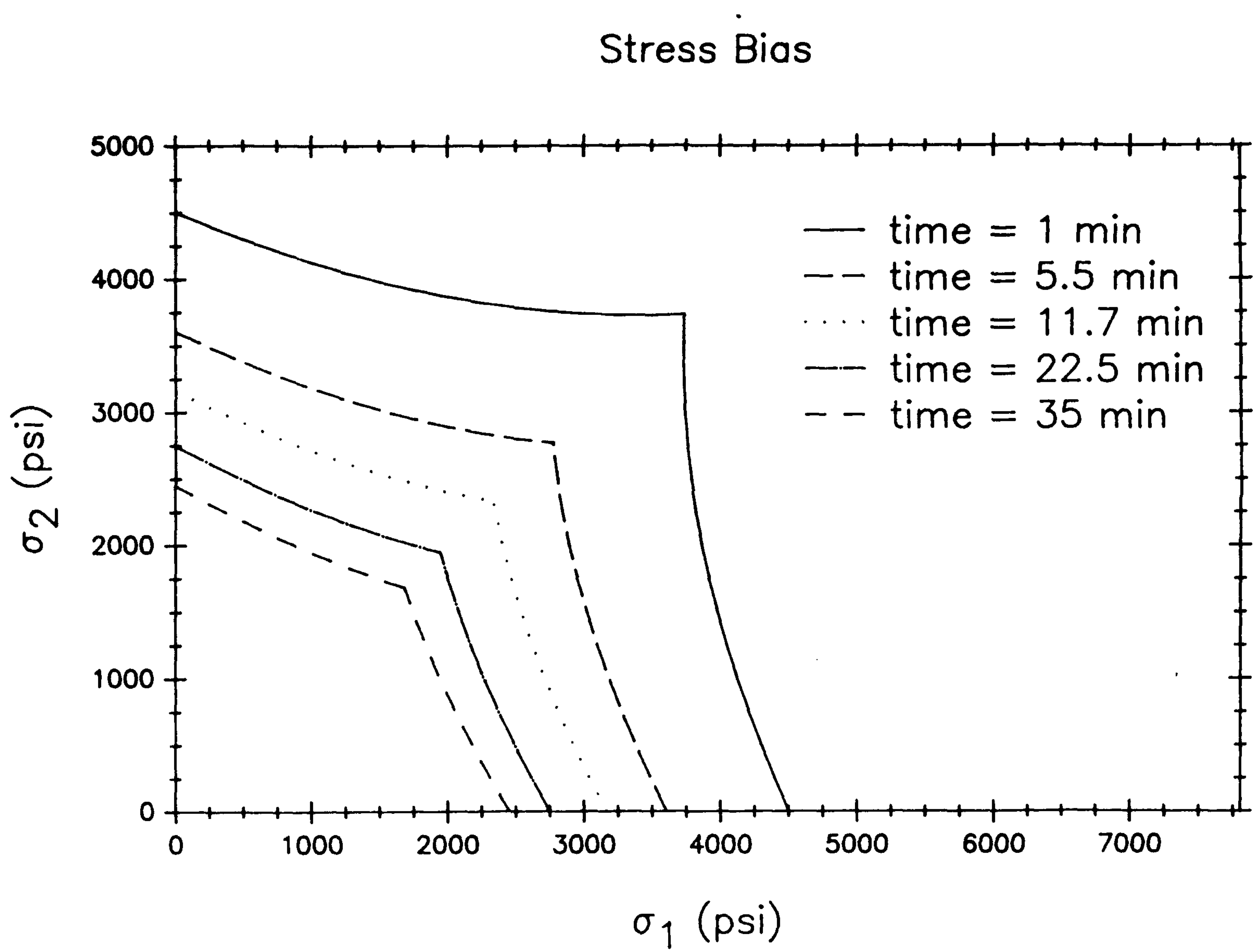

Figure 4.3. Best Fit Semi-Empirical Stress Bias Craze Initiation Criteria for Uniaxial and Biaxial Chemical Craze Data.

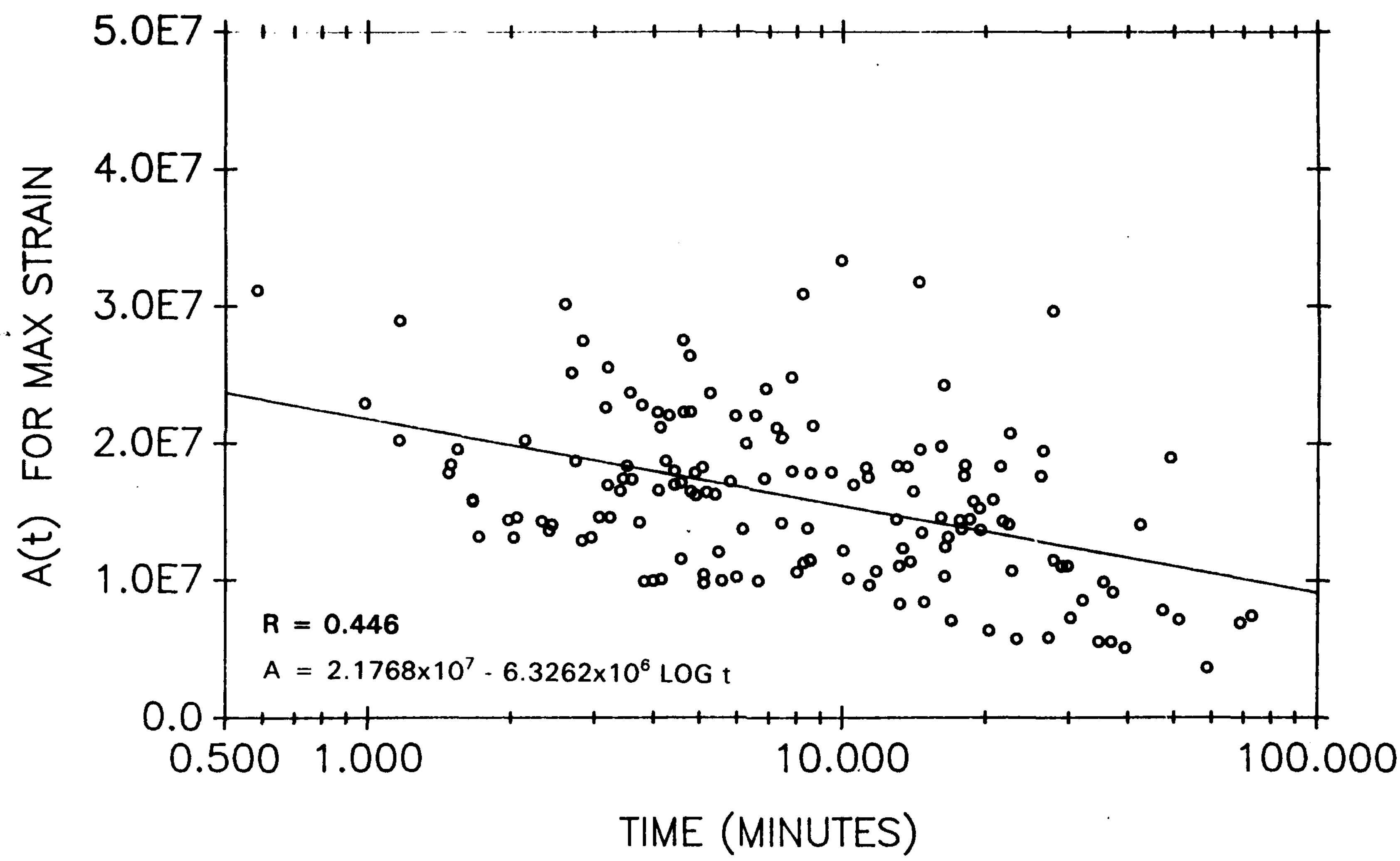

Figure 4.4. Parameter A as a Function of Time for Maximum Strain Criteria.

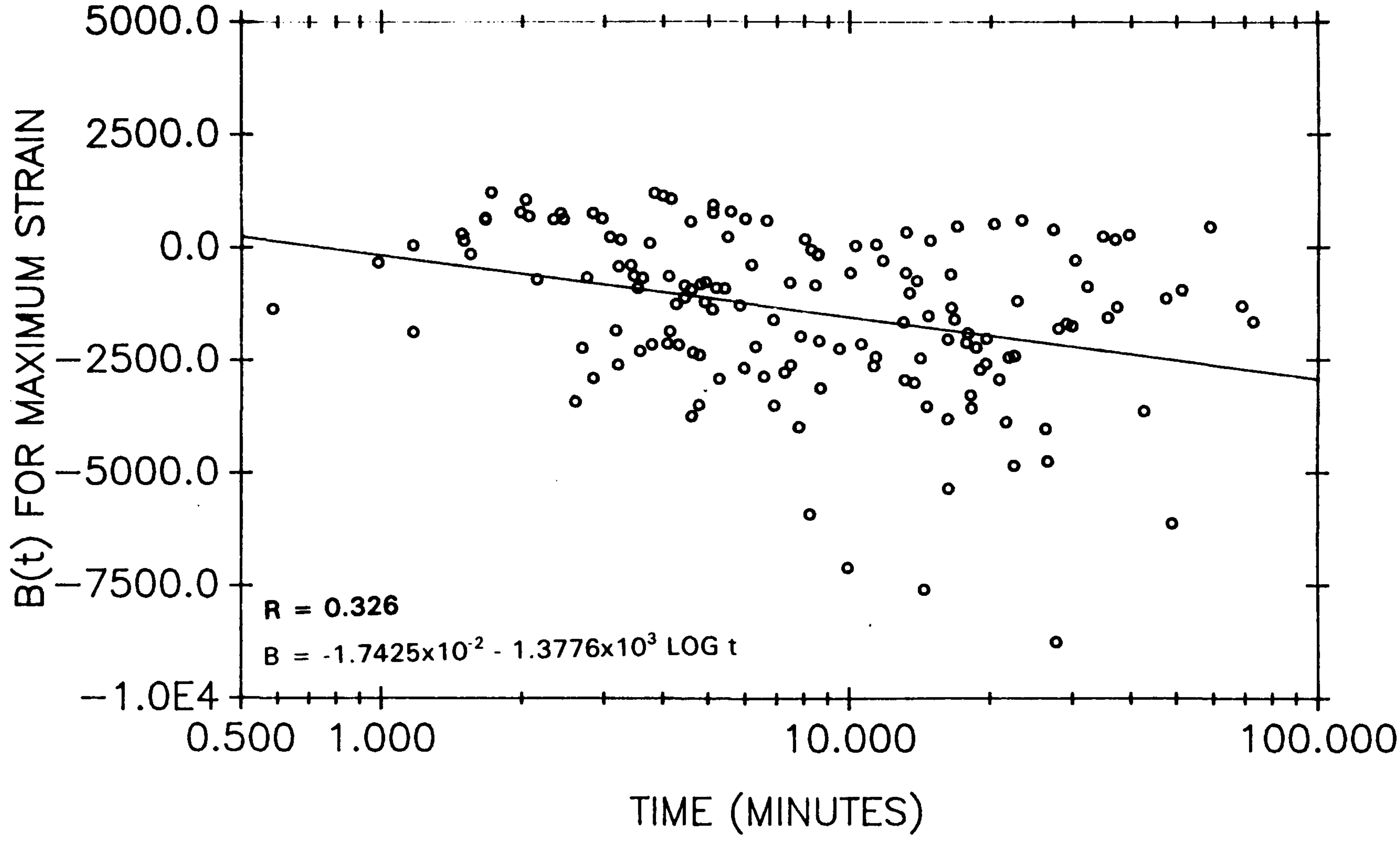

Figure 4.5. Parameter B as a Function of Time for Maximum Strain Criteria.

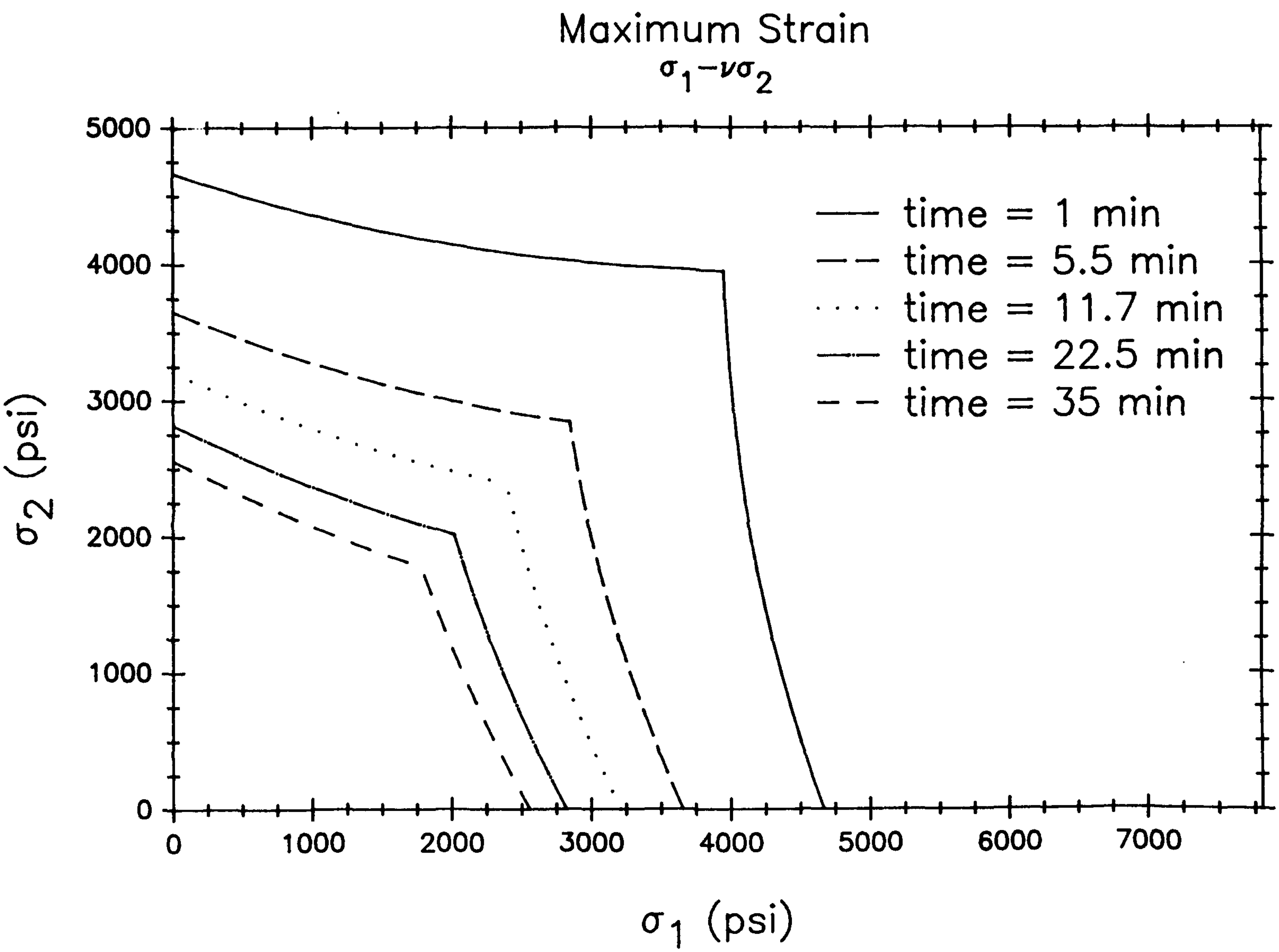

Figure 4.6. Best Fit Semi-Empirical Maximum Strain Craze Initiation Criteria for Uniaxial and Biaxial Chemical Craze Data.

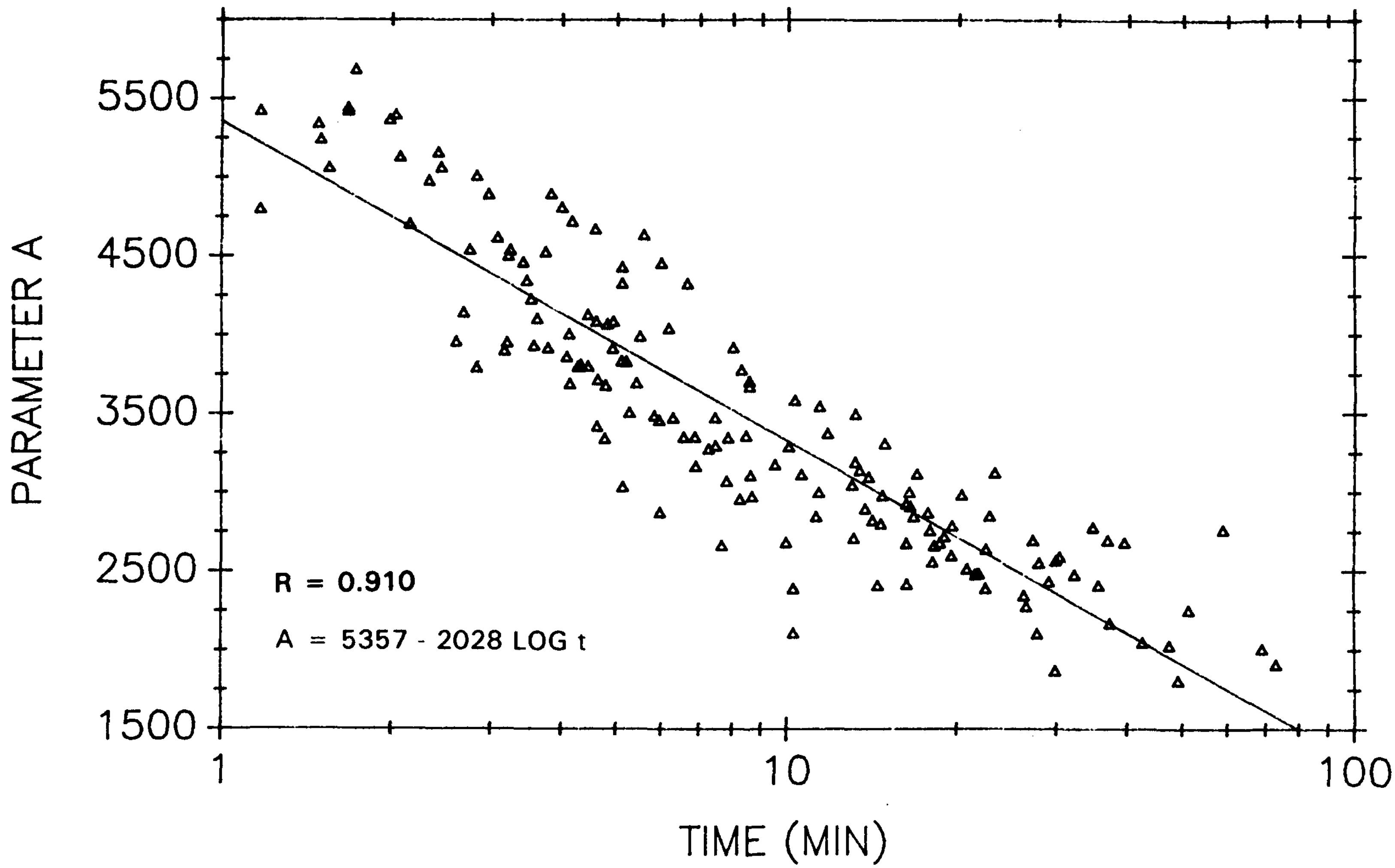

Figure 4.7. Parameter A as a Function of Time for Elliptical Shaped Craze Initiation Criteria Curves.

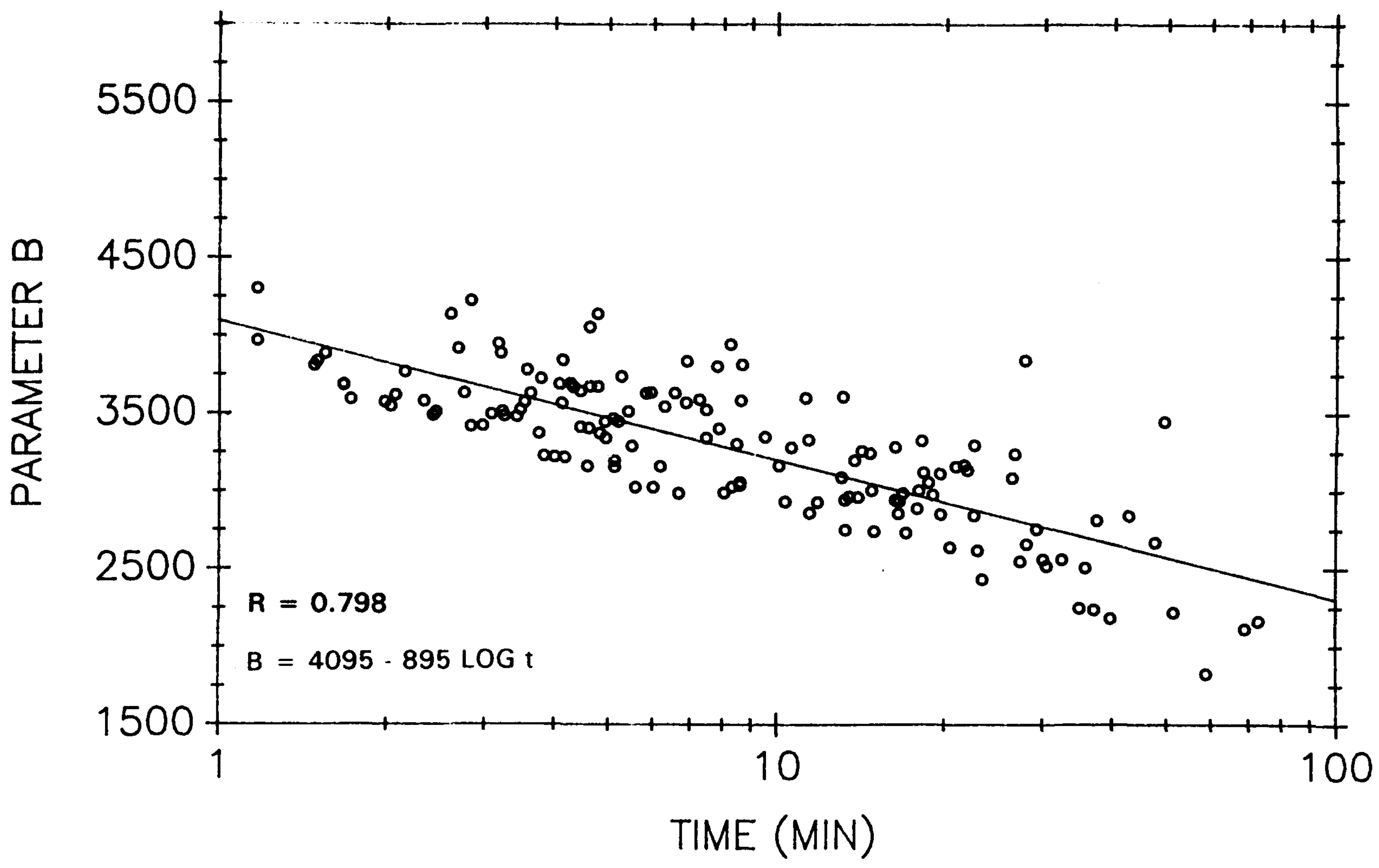

Figure 4.8. Parameter B as a Function of Time for Elliptical Shaped Craze Initiation Criteria.

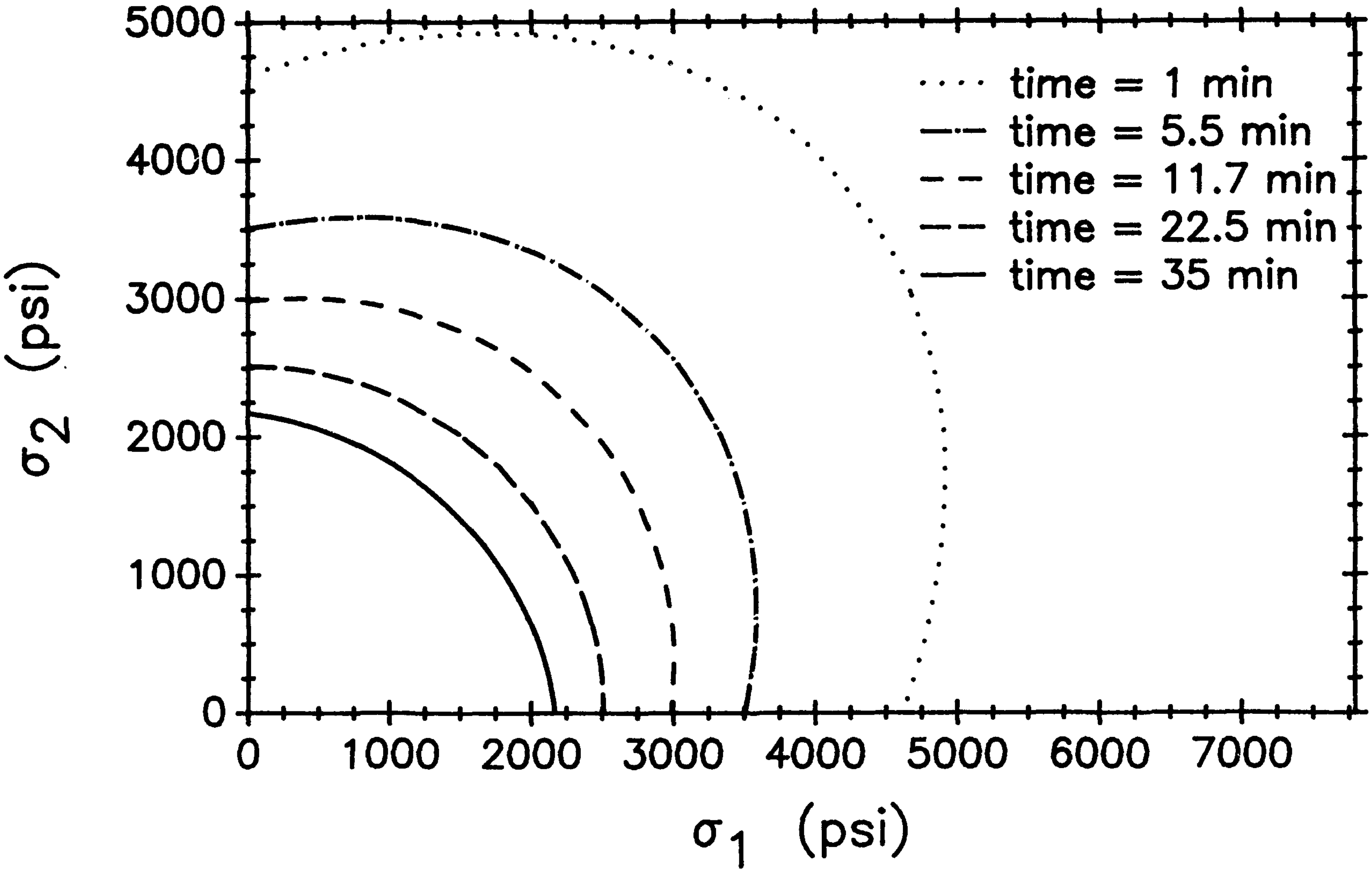

Figure 4.9. Best Fit Empirical Elliptical Craze Initiation Criteria for Uniaxial and Biaxial Chemical Craze Data.

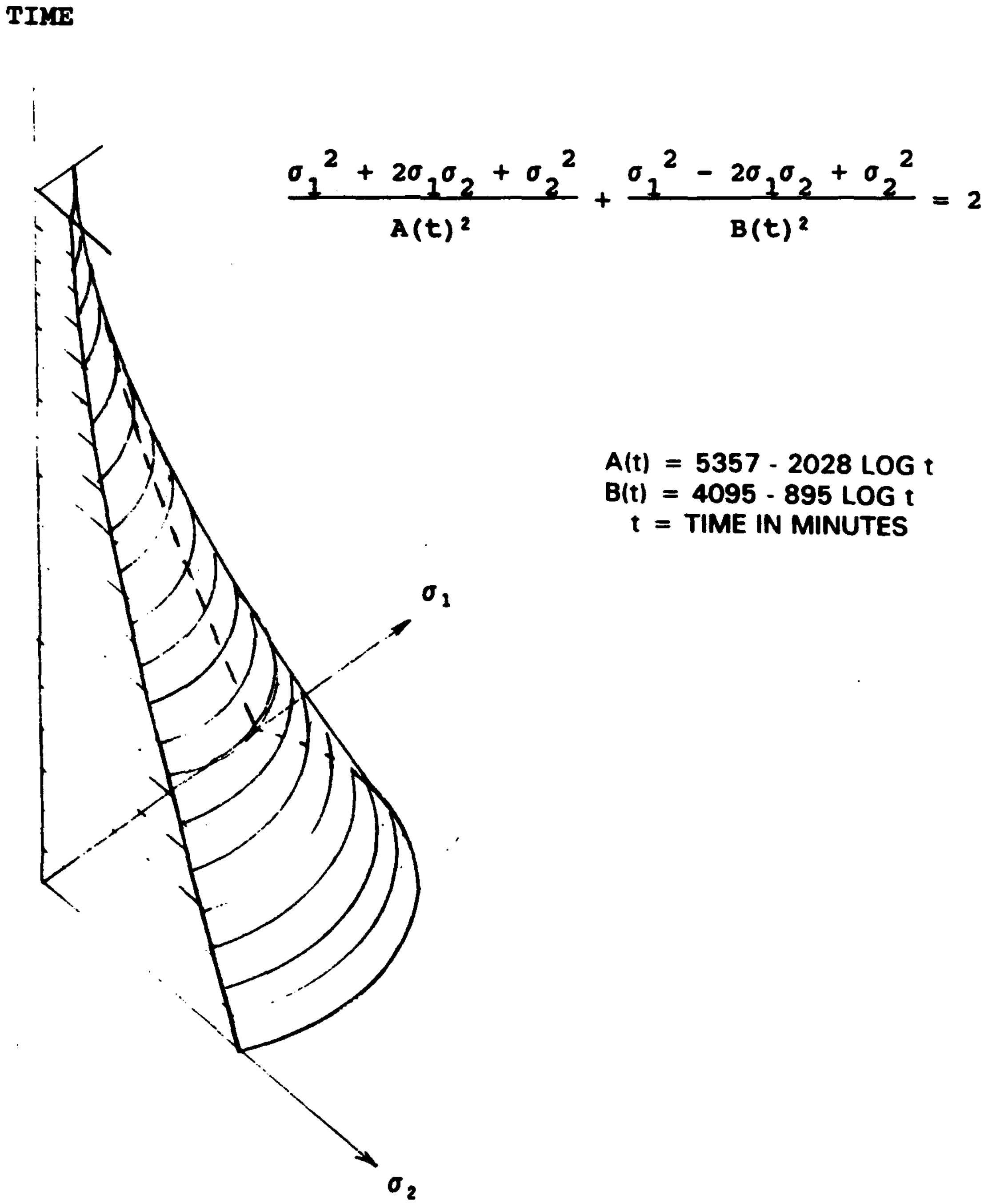

Figure 4.10. Elliptical Craze Initiation Criteria in Biaxial Stress and Time Space.

Table 4.1 presents the equations for each of the three proposed criterion, the values of the parameters for each equation, and the corresponding coefficient of determination, R, for each parameter. The elliptical stress craze initiation criterion provides the best fit to the data obtained, with R values for the two parameters of 0.8 and 0.9.

TABLE 4.1

SUMMARY OF PROPOSED CRAZE INITIATION CRITERION

CRAZE INITIATION CRITERION	EQUATION	PARAMETER A	COEFFICIENT OF DETERMINATION R	PARAMETER B	COEFFICIENT OF DETERMINATION R
Stress Bias Criterion	$\sigma_1 - \sigma_2 \geq A/(\sigma_1 + \sigma_2) + B$	$A = 5.115 \times 10^7 - 1.881 \times 10^7 \log t$	0.730	$B = -6.8519 \times 10^3 + 1.8488 \times 10^2 \log t$	0.033
Maximum Strain Criterion	$\sigma_1 - \mu\sigma_2 = A/(\sigma_1 + \sigma_2) + B$	$A = 2.1768 \times 20^7 - 6.3262 \times 10^6 \log t$	0.446	$B = -1.7425 \times 10^{-2} - 1.3776 \times 10^3 \log t$	0.326
Elliptical Criterion	$(\sigma_1^2 + 2\sigma_1\sigma_2 + \sigma_2^2)/A^2 + (\sigma_1^2 - 2\sigma_1\sigma_2 + \sigma_2^2)/B^2 = 2$	$A = 5.357 \times 10^3 - 2.028 \times 10^3 \log t$	0.910	$B = 4.095 \times 10^3 - 8.95 \times 10^2 \log t$	0.798

SECTION 5

DISCUSSION, CONCLUSIONS, AND RECOMMENDATIONS

The results of this program indicate that there is a definite relationship between uniaxial and biaxial chemical stress crazing with isopropyl alcohol. The exact relationship was not determined in this effort. Three possible chemical stress crazing criterion have been presented. Two represent adaptations of criterion which have been developed for pure stress crazing (where the craze agent is air), and the third criterion represents an empirical elliptical criterion. The elliptical craze initiation criterion provided the best fit to the data obtained.

The choice of a circular plate specimen prevented studying craze in all regions of the biaxial stress state. Even though the biaxial craze specimen design used in this effort is more simple to fabricate, test, and analyze than those used by other researchers to study biaxial crazing, it is not possible to study all of the combinations of principle biaxial stresses of interest with this specimen. Therefore, a different type of specimen is required for future analysis of biaxial craze. To better define a multiaxial chemical stress crazing criterion, other tests should be conducted, with different combinations of principle tensile stresses, and with combinations of tensile and compressive stresses.

It is recommended that future work also include analysis of the effects of other chemicals (in addition to isopropyl alcohol) on crazing. In addition to conducting more tests with different combinations of biaxial stresses and with different chemicals, it is recommended that future work also take into account area effects. The testing on this program was conducted with time to initiation as the measured parameter. If future testing were to be conducted with the measured parameter being time to a specified craze density (i.e. number of crazes per surface area) instead of time to initiation of first craze, it would allow a etter comparison of different types of tests. Time to initiation of first craze is a function of the surface area at a given stress level. Crazing occurs sooner on larger areas than smaller ones. The cantilever beam has a given surface area of material at each stress level, while the area at each stress level for the biaxial plate specimen is a function of the radial location in the plate ana is not equal to the area for the cantilever beam specimen. In general, area effects have been ignored by researchers.

REFERENCES

1. Kambour, R. P., "A Review of Crazing and Fracture in Thermoplastics," Journal of Polymer Science, Macromolecular Reviews, Volume 7, 1-154 (1973).

2. Sternstein, S. S. and L. Ongchin, Polymer Preprints, Am. Chem. Soc., Div. Polymer Chem., 10 (2), 1117 (1969).

3. Bowden, P. B. and R. J. Oxborough, "A Critical Strain Criterion for Craze Formation in Polystyrene," Paper, Brit. Plastics Institute, Research Meeting on The Effect of Structure on the Fracture of Plastics; The Role of Craze in Fracture, University of Liverpool, Liverpool, England (April 14, 1972).

 ☆U.S. GOVERNMENT PRINTING OFFICE: 1992 - 648-127/62388